

# PCCP

Accepted Manuscript



This is an *Accepted Manuscript*, which has been through the Royal Society of Chemistry peer review process and has been accepted for publication.

*Accepted Manuscripts* are published online shortly after acceptance, before technical editing, formatting and proof reading. Using this free service, authors can make their results available to the community, in citable form, before we publish the edited article. We will replace this *Accepted Manuscript* with the edited and formatted *Advance Article* as soon as it is available.

You can find more information about *Accepted Manuscripts* in the [Information for Authors](#).

Please note that technical editing may introduce minor changes to the text and/or graphics, which may alter content. The journal's standard [Terms & Conditions](#) and the [Ethical guidelines](#) still apply. In no event shall the Royal Society of Chemistry be held responsible for any errors or omissions in this *Accepted Manuscript* or any consequences arising from the use of any information it contains.

## Compressibility, thermal expansion coefficient and heat capacity of CH<sub>4</sub> and CO<sub>2</sub> hydrate mixtures using molecular dynamics simulations

Cite this: DOI:

F.L. Ning<sup>a</sup>, K. Glavatskiy<sup>b</sup>, Z. Ji<sup>c</sup>, S. Kjelstrup<sup>d,e\*</sup>, T. J. H. Vlugt<sup>e</sup>

Received 00th xx x 2014,  
Accepted 00th xx x 2014

DOI:

[www.rsc.org/](http://www.rsc.org/)

<sup>a</sup> Faculty of Engineering, China University of Geosciences, Wuhan, Hubei, 430074, China.

<sup>b</sup> School of Applied Sciences, RMIT University, Melbourne VIC 3001, Australia.

<sup>c</sup> Faculty of Materials Science and Chemistry, China University of Geosciences, Wuhan, Hubei, 430074, China.

<sup>d</sup> Department of Chemistry, Norwegian University of Science and Technology, 7491- Trondheim, , Norway.

<sup>e</sup> Process & Energy Laboratory, Delft University of Technology, Leeghwaterstraat 39, 2628CB, Delft, The Netherlands.

To understand the thermal and mechanical properties of CH<sub>4</sub> and CO<sub>2</sub> hydrates is essential for the replacement of CH<sub>4</sub> with CO<sub>2</sub> in natural hydrate deposits as well as for CO<sub>2</sub> sequestration and storage. In this work, we present isothermal compressibility, isobaric thermal expansion coefficient and specific heat capacity of fully occupied single-crystal sI-CH<sub>4</sub> hydrates, CO<sub>2</sub> hydrates and hydrates of their mixture using molecular dynamics simulations. Eight rigid/nonpolarisable water interaction models and three CH<sub>4</sub> and CO<sub>2</sub> interaction potentials were selected to examine the atomic interactions in the sI hydrate structure. The TIP4P/2005 water model combined with the DACNIS united-atom CH<sub>4</sub> potential and TraPPE CO<sub>2</sub> rigid potential were found to be suitable molecular interaction models. Using these molecular models, the results indicate that both the lattice parameters and the compressibility of the sI hydrates agree with those from experimental measurements. The calculated bulk modulus for any mixture ratio of CH<sub>4</sub> and CO<sub>2</sub> hydrates varies between 8.5 GPa and 10.4 GPa at 271.15K between 10-100MPa. The calculated thermal expansion and specific heat capacities of CH<sub>4</sub> hydrates are also comparable with experimental values above approximately 260 K. The compressibility and expansion coefficient of guest gas mixture hydrates increase with an increasing ratio of CO<sub>2</sub>-to-CH<sub>4</sub>, while the bulk modulus and specific heat capacity exhibit the opposite trend. The presented results for the specific heat capacities of 2220-2699.0 J/kg.K for any mixture ratio of CH<sub>4</sub> and CO<sub>2</sub> hydrates are the first reported so far. These computational results provide a useful database for practical natural gas recovery from CH<sub>4</sub> hydrates in deep oceans where CO<sub>2</sub> is considered to replace CH<sub>4</sub>, as well as for phase equilibrium and mechanical stability of gas hydrate-bearing sediments. The computational schemes also provide an appropriate balance between computational accuracy and cost for predicting mechanical and thermal properties of gas hydrates in the high temperature range ( $\geq 260$  K), and the schemes may be useful for the study of other complex hydrate systems.

**Keywords:** gas hydrate; compressibility; thermal expansion; heat capacity; molecular dynamics simulations

\* Corresponding author: [signe.kjelstrup@ntnu.no](mailto:signe.kjelstrup@ntnu.no)

## 1. Introduction

Gas hydrates, also known as clathrate hydrates, are ice-like crystals in which gas molecules (the guest) are encapsulated in a network (the host) formed by hydrogen-bonded water molecules. Commonly investigated guest molecules are the components of natural gas, such as CH<sub>4</sub>, CO<sub>2</sub><sup>1-2</sup>. There are three typically known hydrate structures: structures: I (sI), II (sII), and H (sH)<sup>3</sup>. CH<sub>4</sub> and CO<sub>2</sub> normally form the sI hydrate if pressure is not extreme (normally  $\leq 100$  MPa). Research work on clathrates has grown tremendously since gas hydrates were discovered in the permafrost regions and in deep ocean deposits<sup>4</sup>. They have drawn great attention from academics, industry, and government due to their importance for flow assurance<sup>5-6</sup>, energy storage (including hydrogen energy)<sup>7-8</sup>, as a potential source<sup>9</sup>, for environmental impacts (including marine biology and outer space explorations)<sup>10-13</sup>, as well as for applications such as cold storage<sup>14</sup>, seawater desalination<sup>15-16</sup>, and even disease treatment by gas-hydrate-based medicine in plasters or pills<sup>17</sup>.

With the increasing realization of CH<sub>4</sub> hydrates as a potential energy source as well as CO<sub>2</sub> hydrates as a candidate for production of gas from CH<sub>4</sub> hydrate deposits and CO<sub>2</sub> storage in deep oceans<sup>18-19</sup> (In fact, CH<sub>4</sub> recovery by CO<sub>2</sub> exchange is one kind of means for CO<sub>2</sub> storage in deep oceans), understanding of mechanical and thermal properties such as compressibility and heat capacity of CH<sub>4</sub> and CO<sub>2</sub> hydrates, becomes important. The basic information is critical for gas storage and transportation, safe gas and water recovery from natural deposits of gas hydrates in the earth, even for processes on other planets. For example, knowledge of the compressibility and the thermal expansion coefficient are needed for geophysical modelling of seismic data and evaluations of mechanical stability risks at CO<sub>2</sub> storage and CH<sub>4</sub> hydrate production<sup>17</sup>. The heat capacity of CH<sub>4</sub> hydrate is a key for modelling controlled production of CH<sub>4</sub> from hydrate and hazard mitigation in conventional hydrocarbon extraction<sup>20</sup>.

Most of the thermal and mechanical properties of gas hydrates by far are found to be close to that of ice  $I_h$  because of the similar hydrogen-bonded network. Distinctive physical properties of gas hydrates are the thermal conductivity and the thermal expansion coefficient<sup>21</sup>. At 0 °C, the thermal conductivity of a clathrate hydrate is anomalously low as compared to ice, and more surprising, the temperature dependence is characteristic for an amorphous material<sup>22</sup>. Below 200 K, thermal expansion coefficients are much larger than that of ice  $I_h$ <sup>21</sup>. To understand these anomalous properties, many studies<sup>21-28</sup> were conducted and it was concluded that the thermal conductivity and expansion of gas hydrates depend on the structure of cages, guest type and size, and the occupancy. The host-host interactions play the same important role for the thermal conductivity and the thermal expansion coefficient of gas hydrates compared to the guest-host coupling interaction. In terms of the compressibility of gas hydrates, neutron diffraction and hard-X-ray synchrotron diffraction have been utilized to investigate the cage occupancy and isothermal compressibility of N<sub>2</sub>-, O<sub>2</sub>-, air-clathrates, hydrogenated and deuterated CH<sub>4</sub> hydrates<sup>29-31</sup>. It was found that the unit cell parameters of these hydrates appeared to be determined not only by the size, shape and number (single or double occupation) of the guest molecules in the cages but also by the strength of molecular interactions. Up to now, measurements have been conducted to explore the compressibility<sup>29-31</sup>, thermal expansion coefficient<sup>21,32-38</sup> and heat capacity<sup>20,39-42</sup> of clathrate

hydrates. However, published data of these physical properties are still relatively rare and obtained in a rather narrow range of temperatures and pressures. Measuring such properties is also rather difficult, time-consuming and costly<sup>6</sup>. The outcomes of the measurements strongly depend on the purity of hydrate samples. Residual water and gas, even the potential presence of ice or micro pores in the samples, can significantly affect the accuracy of the measurements.

In addition, a huge amount of macro-, meso- and micro-scopic experiments have been carried out to grasp the general properties of gas hydrates<sup>6</sup>. Some fundamental issues such as the effect of host-guest, guest-guest interaction on certain properties, the mechanism of nucleation, dissociation, and inhibition, however, remain poorly understood, and are even confusing to some extent<sup>43</sup>. This has motivated us to use molecular dynamics (MD) simulations in the studies of mechanical and thermal properties of gas hydrates. MD simulations have been demonstrated to be a powerful tool to probe the nature of gas hydrates on a molecular scale and link the microscopic behaviour to macroscopic properties<sup>15-16,44</sup>. Since the first MD simulation on gas hydrates was performed by Tse et al. in 1983<sup>45</sup>, the literature on this topic counts more than 500 scientific papers. The simulation time and system size have also increased from 30 ps and a single cubic unit cell of a hydrate (containing 46 water molecules)<sup>45</sup> to 5  $\mu$ s<sup>46</sup> and 90 unit cells (containing 4,140 water molecules)<sup>47</sup>. In general, MD simulations have been used to study the physical properties, mechanisms of formation and dissociation, kinetic inhibition, stability, as well as hydrogen storage and CO<sub>2</sub> sequestration<sup>16,44</sup>. MD simulations were able to validate experimental reports on the thermal conductivity and explained why hydrates behave differently from ice<sup>22,26,48</sup>.

However, studies of isothermal compressibility and isobaric heat capacity of CH<sub>4</sub> and CO<sub>2</sub> hydrates by MD simulation method have been fewer. It is important to better understand how the two types of hydrates will behave when exposed to pressure and temperature fields. This is critical for exchange of CH<sub>4</sub> by CO<sub>2</sub> in hydrate deposits. The difference between mechanical properties of CH<sub>4</sub> and CO<sub>2</sub> hydrates may induce the risks of sediment deformations, and temperature variation which depend on the system heat capacity can affect the exchange rate. In addition, the limitations of the van der Waals-Platteeuw (vdWP) model for hydrate equilibrium are, at least in part, due to the fact that it does not account for hydrate volume (i.e., lattice parameter) variations with guest type, temperature, or pressure<sup>21</sup>. Studies have demonstrated that a small volume variation in a hydrate lattice (*e.g.*, 1.5%) can lead to significant differences in predicted hydrate formation conditions<sup>49-50</sup>. Therefore, the vdWP model should be modified to incorporate a variable hydrate volume, like was done by Ballard<sup>51</sup>. Systematic measurements on gas hydrate lattice parameters are required if one wants to achieve better thermodynamic predictions of hydrate phase equilibria over wide temperature and pressure ranges. Also, the nature of molecular interactions responsible for the volume variation needs to be identified. It may also be useful to know the origin of this variation. This provides yet a motivation for the present study. We compare several water models and guest intermolecular potentials, to find which combination can predict the suitable lattice parameters of CH<sub>4</sub> and CO<sub>2</sub> hydrates over a wide temperature and pressure range. We then proceed to report results on calculations of the isothermal compressibility, the thermal expansion coefficient and the heat capacity for the sI structure, fully filled with CH<sub>4</sub>, CO<sub>2</sub> and their mixtures, all using MD simulations.

## 2. Simulation methods

### 2.1. Simulation tool and system definition

Isotropic NPT MD simulations with the Nosé-Hoover barostat algorithm<sup>52-53</sup> modified by Melchionna et al.<sup>54</sup> and NVT MD simulations with the Nosé-Hoover thermostat algorithm<sup>53</sup> were performed on a supercell of CH<sub>4</sub> and CO<sub>2</sub> hydrates<sup>55</sup>. The cubic system consisted of 3×3×3 unit cells (36.09×36.09×36.09 Å initial dimensions, i.e., lattice parameter of a unit cell is 12.03 Å<sup>56</sup>) and had periodic boundary conditions. The starting configuration of the water oxygen atoms for all simulations was acquired from sI structural information obtained by X-ray diffraction experiments<sup>56</sup>. The initial orientations of the water molecules were assigned at random, and subsequently, a short Monte Carlo simulation was performed to adjust the orientation for consistency with the Bernal-Fowler rule<sup>57</sup>. Next, CH<sub>4</sub> and CO<sub>2</sub> molecules were placed approximately at the centre of the water cages. The supercell consisted of 1242 water molecules and 216 (full occupancy) CH<sub>4</sub> and/or CO<sub>2</sub> molecules (i.e., the hydrate number is 5.75). Thermostat and barostat relaxation times of 0.5 and 2.0 ps were used, respectively. The equations of motion were integrated with a time step of 1 fs using the Verlet leapfrog algorithm<sup>58</sup>. The Coulombic long-range interactions were calculated using the Ewald summation method<sup>58</sup> with a relative precision of 1×10<sup>-6</sup>, and all intermolecular interactions in the simulations were calculated with a cutoff distance of  $R_{\text{cutoff}} = 12.0$  Å.

### 2.2 Computational procedure

MD simulations were first performed with all eight water models (SPC/E, TIP3P, TIP4P, TIP4PEw, TIP4PIce, TIP4P2005, TIP5P and TIP5P) combined with all three CH<sub>4</sub> interaction potentials (OPLS-UA, DACNIS-UA and TKM-AA) to evaluate the ability of the model pairs to predict stable sI CH<sub>4</sub> hydrates by investigating the radial distribution functions (RDFs) at 271.15 K and 5 MPa (see the Supporting Information). At the temperature and pressure, the methane hydrate should keep stable because equilibrium pressure of methane hydrates at 271K is about 2.4 MPa according to the hydrate prediction programs CSMHYD<sup>51</sup>. Except for the TIP3P water model hydrates, the calculated RDFs of the other seven water model hydrates were in agreement with experiments and other MD simulations<sup>59-60</sup>. The first two peaks of  $g_{OO}(r)$  are at approximately 2.78 Å and 4.5 Å, which indicates the existence of tetrahedral hydrogen bonding structures of H<sub>2</sub>O molecules in CH<sub>4</sub> hydrates<sup>60</sup>. These results imply that all water models except TIP3P and three CH<sub>4</sub> potentials can describe the corresponding hydrate structures under conditions of hydrate stability (see Figure S1 and S2 in the Supporting Information).

Next, we identified the water model and CH<sub>4</sub> potential that could best reproduce the lattice parameters observed in the experiments at different pressures. To simulate the pressure dependence of the lattice parameters, the temperature was set to the same value of 271.15 K, and the pressure was varied from 10 to 100 MPa in steps of 10 MPa. The upper limit for this pressure is well below the pressure that may promote a structure change because some experiments have shown that the sI type hydrate can transform to the sII type when the pressure is higher than 100 MPa<sup>61-63</sup>. In most cases, these pressures also fall within the range in which the natural gas industry operates<sup>64</sup>. To simulate the temperature-dependent

lattice parameters, the pressure was set to atmospheric pressure or 20 MPa, while the temperature varied from 80 to 250 K. According to the first step of the simulation procedure, the configuration energy actually changed very slowly after 500 ps and is stable after approximately 3 ns. We therefore decreased the simulation time from 6 ns to 3 ns and selected an equilibration time of 500 ps. The average lattice parameters of CH<sub>4</sub> hydrates described by different water models and CH<sub>4</sub> potentials were obtained and compared with the corresponding experimental values. Thus, a suitable combination of the water model and CH<sub>4</sub> potential can be obtained. For CO<sub>2</sub> hydrate, the rigid three-site TraPPE, EPM and EPM2 potentials were selected for comparison, and determination of a suitable CO<sub>2</sub> potential (the detailed information is given in the Supporting Information).

To reproduce the lattice parameters observed in experiments, the size parameters of the LJ interaction were retained, while the energetic parameters of the LJ host-guest interaction were rescaled. That is, the standard Lorentz-Berthelot rule was transformed into the following expression<sup>65</sup>:

$$\varepsilon_{ij} = \lambda \cdot (\varepsilon_{ii} \varepsilon_{jj})^{1/2} \quad (1)$$

where  $\lambda$  is a rescaled parameter. When  $\lambda=1$ , Equation (1) is reduced to the standard Lorentz-Berthelot rule. To determine a suitable value of  $\lambda$ , similar simulations with a particular host and a particular guest model were performed.

Finally, using the particular host and guest model and the adjusted host-guest potential, a series of similar NPT simulations were performed to determine the average lattice parameters and to calculate the corresponding isothermal compressibility and thermal expansion. In these NPT simulations, the simulation time was increased to 7 ns, and the system obtained relatively stable parameters with the shortest computational time (see the Supporting Information). These simulations were performed for fully occupied CH<sub>4</sub> hydrates, CO<sub>2</sub> hydrates and binary hydrates with varying percentages of CH<sub>4</sub> and CO<sub>2</sub> at various temperatures and in the pressure range of 10-100 MPa. The properties were obtained by numerical differentiation according to the following definitions:

$$\kappa_T = -\frac{1}{V} \left( \frac{\partial V}{\partial P} \right)_T \quad (2)$$

$$\alpha_p = \frac{1}{V} \left( \frac{\partial V}{\partial T} \right)_p \quad (3)$$

where  $\kappa_T$  is the isothermal compressibility coefficient, Pa<sup>-1</sup>;  $\alpha_p$  is the thermal expansion coefficient, K<sup>-1</sup>;  $P$  is the pressure, MPa;  $T$  is the temperature, K; and  $V$  is the volume, Å<sup>3</sup>.

Furthermore, we also used the fluctuations in the NPT ensemble to calculate the isothermal compressibility, thermal expansion coefficients and heat capacity of the single-crystal sI hydrates and compared these values with the numerical differentiation method and experimental values. The equations for the fluctuations are as follows<sup>66</sup>:

$$\beta_T = \frac{1}{k_B T \langle V \rangle} \left( \langle V^2 \rangle - \langle V \rangle^2 \right)_{NPT} \quad (4)$$

$$\alpha_p = \frac{\left[ \langle V \cdot U \rangle - \langle V \rangle \cdot \langle U \rangle + P \left( \langle V^2 \rangle - \langle V \rangle^2 \right) \right]_{NPT}}{k_B T^2 \langle V \rangle} \quad (5)$$

$$C_p = \frac{ik_B N}{2} + \frac{1}{k_B T^2} \left[ \begin{array}{l} (\langle U^2 \rangle - \langle U \rangle^2) + \\ 2P(\langle V \cdot U \rangle - \langle V \rangle \cdot \langle U \rangle) \\ + P^2(\langle V^2 \rangle - \langle V \rangle^2) \end{array} \right]_{NPT} \quad (6)$$

where  $\beta_T$  is the bulk modulus, Pa;  $k_B$  is Boltzmann's constant and equal to  $1.38 \times 10^{-23}$  J/K;  $U$  is the potential energy, J;  $C_p$  is the heat capacity, J/K;  $i$  is the number of degrees of freedom; and  $N$  is the number of molecules. The first term of Eqs.(6) represents the contribution from the kinetic energy, and for monoatomic gases,  $i = 3$ . For a rigid  $\text{CO}_2$  molecule,  $i = 5$ . Therefore, the first term of Equation (6) can be expressed as follows:

$$\frac{i}{2} k_B N = \frac{i}{2} k_B N_{H_2O} + \frac{3}{2} k_B N_{CH_4} + \frac{5}{2} k_B N_{CO_2} \quad (7)$$

where  $i$  represents the number of degrees of freedom (DOF) of water molecules,  $N_{H_2O}$  is the number of water molecules,  $N_{CH_4}$  is the number of methane molecules and  $N_{CO_2}$  is the number of carbon dioxide molecules. If the water molecules are fully mobile, then  $i = 6$ . If the water molecules can only rotate or only translate, then  $i = 3$ . If the water molecules are fully immobile, then  $i = 0$ . Here, we use  $i=6$  because the water molecules can rotate and translate slightly in the hydrate structures.

Usually, the heat capacity of gas hydrates is reported not in [J/K] but in [J/(kg.K)] or [J/(mol.K)], *i.e.*, the specific heat capacity. Here, we denote the unit of specific heat capacity by [J/(kg.K)]:

$$c_p = \frac{1000 N_A C_p}{Mn} \quad (8)$$

where  $c_p$  is the specific heat capacity, and  $N_A$  is Avogadro's constant. For an MD cell that consists of  $3 \times 3 \times 3$  unit cells, 1 mol MD cell contains 216 mol  $\text{CH}_4$  or  $\text{CO}_2$  when the gases fully occupy the water cages; thus,  $n=216$ .  $M$  is the molecular weight of the gas hydrate if we assume a stoichiometry of  $\text{CH}_4 \cdot 5.75\text{H}_2\text{O}$  or  $\text{CO}_2 \cdot 5.75\text{H}_2\text{O}$  (full occupancy) for  $\text{CH}_4$  or  $\text{CO}_2$  hydrates, respectively.

### 3. Results and discussions

#### 3.1 Comparison of water models and $\text{CH}_4$ and $\text{CO}_2$ potentials

In Table 1, we compare the lattice parameter and corresponding density of the sI- $\text{CH}_4$  hydrate obtained from MD simulations with different water models and  $\text{CH}_4$  potentials at 271.15 K and 5 MPa. Regardless of the  $\text{CH}_4$  potential, the TIP4Pice model produces a much higher value of the lattice parameter, which is close to the initial lattice parameter, 12.03 Å, and a correspondingly much lower density of the sI- $\text{CH}_4$  hydrate than the experimental value. Furthermore, the TIP5PEw model yields the smallest lattice parameter (the largest density of the  $\text{CH}_4$  hydrate). The SPC/E, TIP4P and TIP4PEw models produce intermediate values, and the TIP4P2005 hydrate has a lattice parameter that is closest to the experimental value (Table 3). In addition, the TIP5P and TIP5PEw hydrates result in essentially the same values; however, the latter can yield a lower average configuration energy. This finding is very similar to the result from the TIP4P and TIP4PEw hydrates. An apparent density increase occurs if the water molecules are modelled by the TIP5P and TIP5PEw models. The geometry of the TIP5P and TIP5PEw models may cause this behaviour because these models are non-planar, whereas the others are planar.

We also investigated the pressure dependency of the lattice parameter of the sI-CH<sub>4</sub> hydrate described by the DACNIS CH<sub>4</sub> potential<sup>67</sup> using different water models. The pressure was increased from 10 to 100 MPa in steps of 10 MPa while keeping the temperature constant (Figure 1). Again, the experimental results were best described by the TIP4P2005 water model. Other simulations also observed that this water model effectively predicted the interfacial properties of vapour/liquid coexistence<sup>68-69</sup>. The stability of the TIP4PIce hydrate was weakly affected by the CH<sub>4</sub> potential, and the lattice parameter deviated greatly from the experimental values and varied little with the pressure, meaning that this model is less suitable for a description of the isothermal compressibility of hydrates. The TIP4PIce model may, however, be suitable for studying the kinetic processes of hydrates, such as nucleation and growth<sup>46</sup>. Although the 3-site SPCE and five-site TIP5P or TIP5PEw were observed to be more appropriate for describing the thermodynamic stability of gas hydrates by other researchers<sup>59,70</sup>, we did not find that these models reproduce the experimental lattice parameters and corresponding densities of sI-CH<sub>4</sub> hydrates very well. The TIP4P and TIP4PEw water models have been successfully used in many computer simulations and are believed to be the most reliable among the pair potentials for predicting water properties<sup>71</sup>.

**Table 1: lattice parameter (L) and density ( $\rho$ ) of fully occupied sI-CH<sub>4</sub> hydrate from seven water models and three CH<sub>4</sub> potentials at 271.15 K, 5 MPa.**

|                             |                             | Water models |         |         |          |           |        |         |
|-----------------------------|-----------------------------|--------------|---------|---------|----------|-----------|--------|---------|
|                             |                             | SPCE         | TIP4P   | TIP4PEw | TIP4PIce | TIP4P2005 | TIP5P  | TIP5PEw |
| CH <sub>4</sub> potential   |                             |              |         |         |          |           |        |         |
| OPLS-UA                     | L (Å)                       | 11.890       | 11.9079 | 11.9075 | 12.001   | 11.961    | 11.751 | 11.746  |
|                             | $\rho$ (g/cm <sup>3</sup> ) | 0.945        | 0.940   | 0.941   | 0.919    | 0.928     | 0.979  | 0.980   |
| DACNIS-UA                   | L (Å)                       | 11.887       | 11.905  | 11.905  | 11.998   | 11.958    | 11.748 | 11.742  |
|                             | $\rho$ (g/cm <sup>3</sup> ) | 0.945        | 0.941   | 0.941   | 0.919    | 0.929     | 0.979  | 0.981   |
| TKM-AA                      | L (Å)                       | 11.877       | 11.894  | 11.895  | 11.990   | 11.949    | 11.740 | 11.734  |
|                             | $\rho$ (g/cm <sup>3</sup> ) | 0.948        | 0.944   | 0.943   | 0.921    | 0.931     | 0.981  | 0.983   |
| Experimental value, Ref. 29 | L (Å)                       |              |         |         | 11.953   |           |        |         |
|                             | $\rho$ (g/cm <sup>3</sup> ) |              |         |         | 0.930    |           |        |         |

If we fix the water model, we can compare the effect of the CH<sub>4</sub> potential on the lattice parameter. The spherically symmetrical CH<sub>4</sub> potentials (OPLS-UA and DACNIS-UA) produce similar results, while the results of the TKM-AA potential differ from the other two. This finding results because the LJ size parameters for OPLS-UA and DACNIS-UA are almost the same, and the energy parameter for DACNIS-UA is only 7% larger than that for OPLS-UA (see Table 2). The lattice parameter of a TIP4P2005 hydrate with a TKM-AA CH<sub>4</sub> potential is closer to the experimental values than is that of OPLS-UA and DACNIS-UA hydrates (Figure 2). The experimental value shows that the average deviation of the lattice parameter of the sI-CH<sub>4</sub> hydrate described by this combination does not exceed 0.005 Å in the pressure range 10-100 MPa, while DACNIS-UA and OPLS-UA hydrates exhibit average deviations of 0.007 Å and 0.009 Å, respectively, at the same conditions. We further observed that the TIP4P2005 hydrate with OPLS-UA or DACNIS-UA reproduces the experimental values of the temperature-dependent lattice parameter better than with the TKM-AA potential (Figure 3). The three interaction potentials exhibit similar variable trends with pressure and temperature, most likely resulting from

the spherically symmetrical CH<sub>4</sub> molecule<sup>59</sup>. Although the TIP4P2005 CH<sub>4</sub> hydrate with the TKM-AA CH<sub>4</sub> potential provides a better prediction of the pressure behaviour of the sI-hydrate lattice constant at a given temperature, the thermal expansion of CH<sub>4</sub> hydrate under atmospheric pressure reproduced by this combination is not in agreement with experimental data. In addition, the configuration energy in the TKM-AA model is larger than that in the other two models and consumes more computational time (25% more than the OPLS-UA and DACNIS-UA potentials). Therefore, in general, the combination of the TIP4P2005 water model with the DACNIS-UA potential can achieve a balance between relatively accurate lattice parameters and low computational time, which may be useful for MD simulations of the thermal expansion coefficient and isothermal compressibility of gas hydrates.

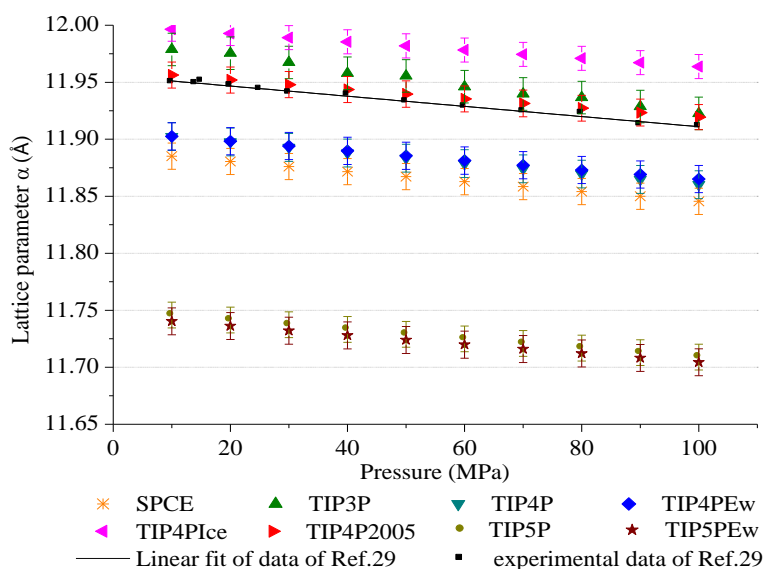


Figure 1. The lattice parameter of the sI-CH<sub>4</sub> hydrate as a function of pressure for different water models with the DACNIS-UA CH<sub>4</sub> potential at 271.15 K compared with experimental results. The errors of the individual calculations were in the range of 0.011-0.014 Å.

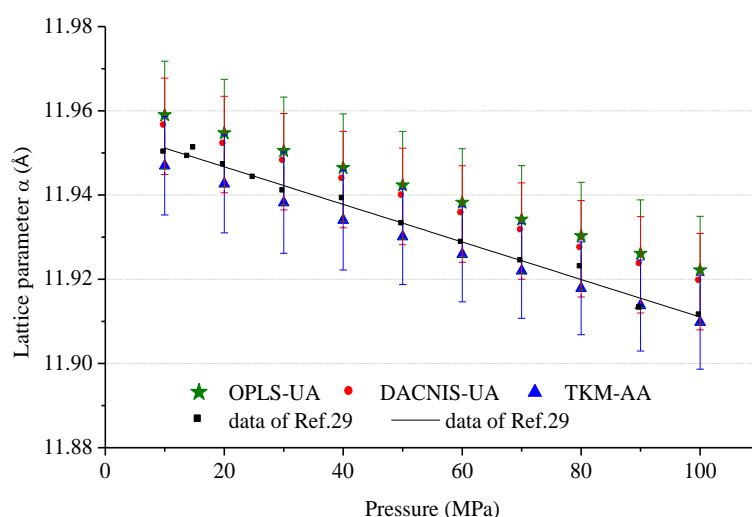


Figure 2. The lattice parameter of the sI-CH<sub>4</sub> hydrate as a function of pressure for TIP4P2005 hydrates at 271.15 K with different CH<sub>4</sub> potentials compared with experimental results. The errors of the individual calculations were in the range of 0.011-0.013 Å.

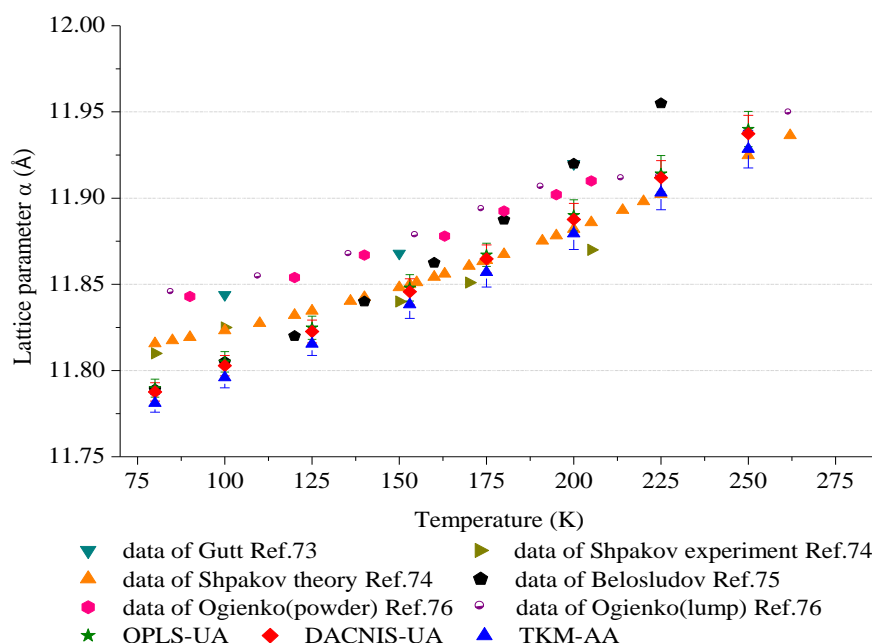


Figure 3. The lattice parameter as a function of temperature under atmospheric pressure for TIP4P2005 hydrates with different  $\text{CH}_4$  potentials. Experimental data are also shown. The errors of the individual calculations were in the range of 0.002-0.006 Å.

Using the TIP4P2005 water model, we compared the effect of the  $\text{CO}_2$  potential on the lattice parameter of fully occupied  $\text{CO}_2$  hydrates under atmospheric pressure and different temperature conditions. The results plotted in Figure 4 demonstrate that the three  $\text{CO}_2$  potentials reproduce nearly the same lattice parameters of  $\text{CO}_2$  hydrates. Considering that the TraPPE  $\text{CO}_2$  rigid potential model can also provide an accurate description of the vapour-liquid phase behaviour for  $\text{CO}_2$ -alkane mixtures<sup>72</sup>, this model was selected as the  $\text{CO}_2$  potential for the remainder of this study.

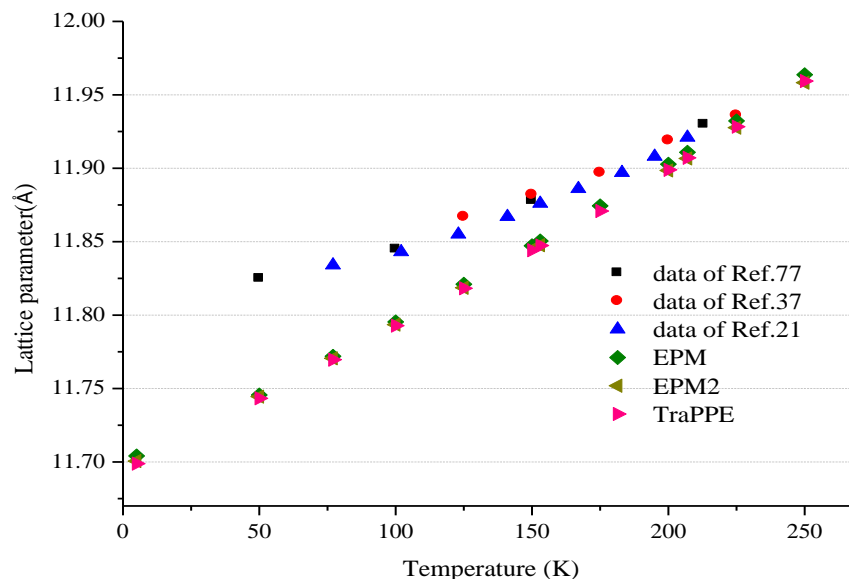


Figure 4. The lattice parameter as a function of temperature under atmospheric pressure for TIP4P2005 hydrates with different  $\text{CO}_2$  potentials. Experimental data are also shown.

From Figures 1-4, it appears that the water models (*i.e.*, host-host interaction) and guest potentials (*i.e.*, guest-guest interaction) both affect the lattice parameter of  $\text{CH}_4$  hydrates, the former more than the latter. Figure 2 demonstrates that

the difference between the simulation results and the experimental values appears to be systematic for the DACNIS-UA potential. This finding suggests that this potential is able to reproduce the lattice parameters observed in the experiments by a modification of only the LJ host-guest interaction. Increasing the energy parameter of the host-guest interaction decreases the lattice parameter of the CH<sub>4</sub> hydrate. Therefore, we rescaled the energy parameter of the LJ host-guest interactions by increasing the  $\lambda$  value in steps of 1% in Equation (1). A value of  $\lambda$  equal to 1.13, resulted in the lattice parameter closest to the experimental value, 11.951 Å at 271.15 K and 10 MPa (Figure 5). Using this optimised value for the host-guest interaction parameter of CH<sub>4</sub> hydrate described by the TIP4P2005 water model and DACNIS-UA CH<sub>4</sub> potential, we again calculated the pressure-dependent lattice parameter at 271.15 K and atmospheric pressure. It was then observed that the pressure-dependent lattice parameters of the CH<sub>4</sub> hydrate deviated from the experimental value by less than 0.002 Å. A similar rescaling of the guest-host interaction parameter did not have a significant effect on the temperature-dependent lattice parameter (Figure 6). This finding may indicate that the effect of the guest-host interaction on the isothermal compressibility is different from the effect on the isobaric thermal expansion coefficient of gas hydrates.

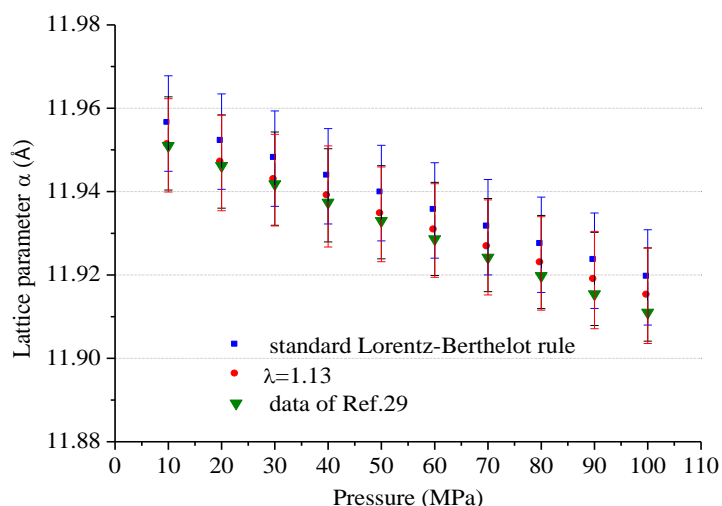


Figure 5. The lattice parameter of sI-CH<sub>4</sub> hydrate as a function of pressure at 271.15 K for TIP4P2005 hydrates with the standard Lorentz-Berthelot rule and rescaled energy parameter for guest-host interaction compared with experimental results. The errors of the individual calculations were in the range of 0.007-0.011 Å.

### 3.2 Isothermal compressibility

The rescaled energy parameter was used for the CH<sub>4</sub>-H<sub>2</sub>O interactions, and a series of simulations to determine the isothermal compressibility was performed. The TIP4P2005 water model was used with the DACNIS-UA CH<sub>4</sub> potential and TraPPE three-site CO<sub>2</sub> potential. The isothermal compressibility of the fully occupied hydrate was investigated as a function of composition, starting with pure CH<sub>4</sub> hydrate and ending with CO<sub>2</sub> hydrate while varying the pressure and temperature. The percentage of CH<sub>4</sub> (CO<sub>2</sub>) in the mixed hydrate represents the percentage of all cages occupied by this guest gas. With an increase in the CO<sub>2</sub> percentage, the lattice parameter of the hydrate increases. This behaviour can be attributed to the large CO<sub>2</sub> molecule, which stretches the hydrate lattice. The corresponding lattice parameters are plotted in Figure 7.

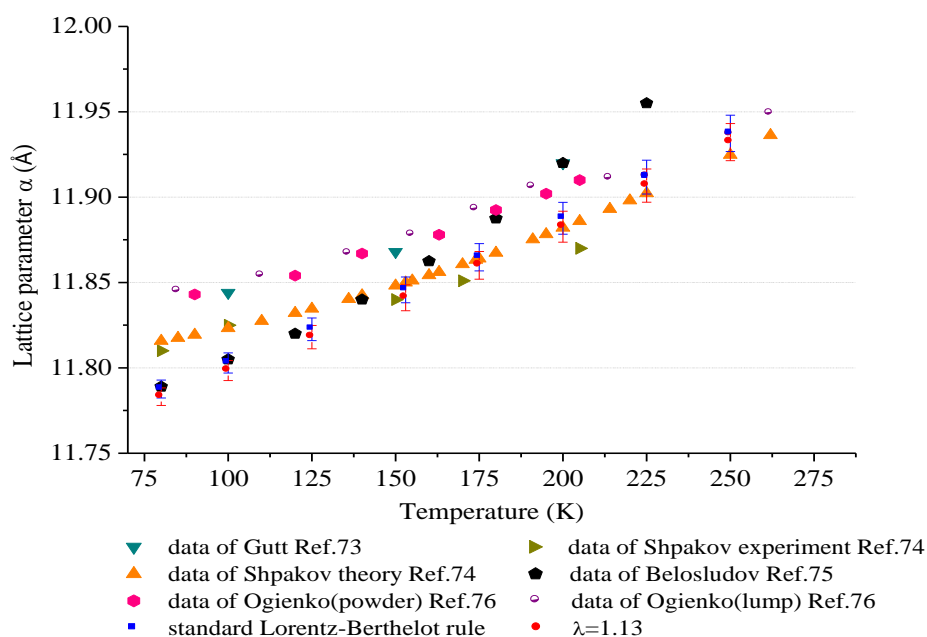


Figure 6. The lattice parameter as a function of temperature under atmospheric pressure for TIP4P2005 CH<sub>4</sub> sI-hydrates with the standard Lorentz-Berthelot rule and rescaled energy parameter for guest-host interaction. The errors of the individual calculations were in the range of 0.003-0.007 Å.

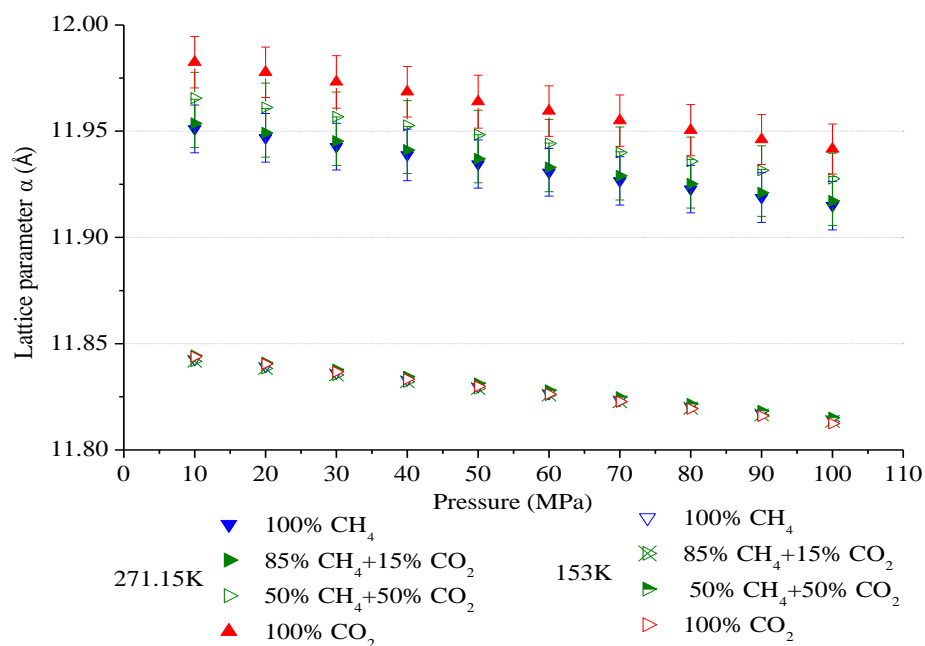


Figure 7. The lattice parameters of sI- CH<sub>4</sub> and CO<sub>2</sub> hydrates as a function of pressure at 271.15 K and 153 K.

The lattice parameters of the fully occupied sI hydrates are seemingly not affected by the guest molecule at low temperatures, such as 153 K. Clearly, the host-guest interaction at low temperature is weak. The data presented in Figure 7 can be fitted to second-order polynomials as follows:

$$\begin{aligned}
 V_{271.15\text{K},100\% \text{CH}_4} &= 9.19456 \times 10^{-5} P^2 - 0.18152 P + 1708.7625 \\
 V_{271.15\text{K},85\% \text{CH}_4+15\% \text{CO}_2} &= 7.91892 \times 10^{-5} P^2 - 0.18149 P + 1709.8249 \quad (3 \leq P \leq 100 \text{ MPa}) \\
 V_{271.15\text{K},50\% \text{CH}_4+50\% \text{CO}_2} &= 6.55428 \times 10^{-5} P^2 - 0.18744 P + 1715.0064 \\
 V_{271.15\text{K},100\% \text{CO}_2} &= 7.38637 \times 10^{-5} P^2 - 0.20274 P + 1722.4441 \\
 V_{153\text{K}} &= 6.51883 \times 10^{-5} P^2 - 0.13911 P + 1662.2903
 \end{aligned} \tag{9}$$

where  $V$  is the volume of the unit cell of the sI hydrate, in  $\text{\AA}^3$ , and  $P$  is the pressure, in MPa. Using these expressions and Equation 2, we determined the isothermal compressibility. Figure 8 provides the values of the compressibility of the fully occupied  $\text{CH}_4$  and  $\text{CO}_2$  sI-hydrates using the numerical differentiation of Equation 9 and fluctuations in the  $NPT$  ensemble (Equation 4). The results from the fit to the polynomial and from the fluctuation method agree relatively well. With an increase in the  $\text{CO}_2$  percentage, the compressibility of the mixed hydrate increases. The isothermal compressibility of a 100%  $\text{CH}_4$  hydrate and a mixed hydrate with 85% are almost the same at low pressures. However, a difference appears at higher pressures. The  $\text{CO}_2$  molecules, which are larger than the  $\text{CH}_4$  molecules, prefer to occupy the large cages, while the  $\text{CH}_4$  molecules are distributed over all the empty spaces. At low pressures, the size of the guest molecule in the large cages has a minor effect on the compressibility. However, at higher pressures, the intermolecular interactions become stronger, and the effect of the size of the guest molecules becomes more pronounced. Figure 8 shows that a gas hydrate occupied by a linear guest molecule appears to be compressed more easily than is one occupied by a symmetric guest molecule; the size of the molecule does not contribute much to the effect.

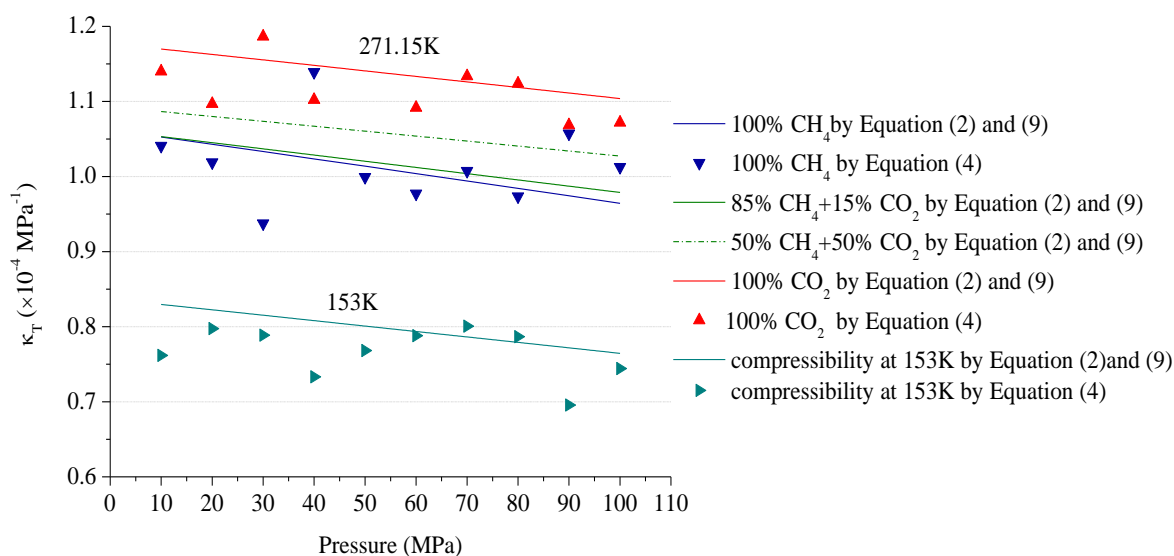


Figure 8. The isothermal compressibility of  $\text{CH}_4$  and  $\text{CO}_2$  hydrates as a function of pressure at 271.15 K and 153 K.

The bulk modulus of the  $\text{CH}_4$  and  $\text{CO}_2$  hydrates is the inverse of the compressibility:

$$\beta_T = \frac{1}{\kappa_T} \tag{10}$$

The bulk modulus of the  $\text{CH}_4$  hydrate from this relation is approximately 9.5 GPa at 271.15 K and 10 MPa, close to the sI  $\text{CH}_4$  hydrate experimental value ( $\approx 9.03$  GPa)<sup>29</sup> at the same temperature. For the  $\text{CO}_2$  hydrate, the bulk modulus varies from 8.5 GPa to 9.1 GPa at the same temperature and 10-100 MPa. With an increase in the  $\text{CO}_2$  percentage, the bulk modulus of the hydrate decreases accordingly. This effect should be considered during  $\text{CH}_4$  recovery from  $\text{CH}_4$  hydrates

in deep oceans by replacing  $\text{CH}_4$  with  $\text{CO}_2$ , especially when the solid  $\text{CH}_4$  hydrates act as cement or have a framework support function in porous sediments. The calculated bulk moduli of  $\text{CH}_4$  hydrates and  $\text{CO}_2$  hydrates are also close to the experimental value of ice ( $I_h$ ), which is approximately 9.097 GPa at 253-268 K<sup>78</sup>. This result, combining Figure 1 and 7, may further indicate that the isothermal compressibility of gas hydrates is primarily determined by the elastic behaviour of the hydrogen-bonded cages, i.e., the host-host interaction plays the primary role in the isothermal compressibility of gas hydrates in the low pressure range.

### 3.3 Isobaric thermal expansion coefficient

We also used the rescaled energy parameter for the  $\text{CH}_4$ - $\text{H}_2\text{O}$  interaction to determine the isobaric expansion coefficient as a function of hydrate composition in a fully occupied sI hydrate at various pressures and temperatures. As potentials, we used the TIP4P2005 water model, DACNIS-UA  $\text{CH}_4$  potential and TraPPE three-site  $\text{CO}_2$  potential. The corresponding lattice parameters are plotted in Figure 9. It is observed that the lattice parameters of the  $\text{CO}_2$  hydrates are smaller than those of  $\text{CH}_4$  hydrates in the low temperature region (for example  $<200$  K); however, they are larger than those of  $\text{CH}_4$  hydrates in the high temperature region ( $>200$  K in this study) at the same pressure conditions.

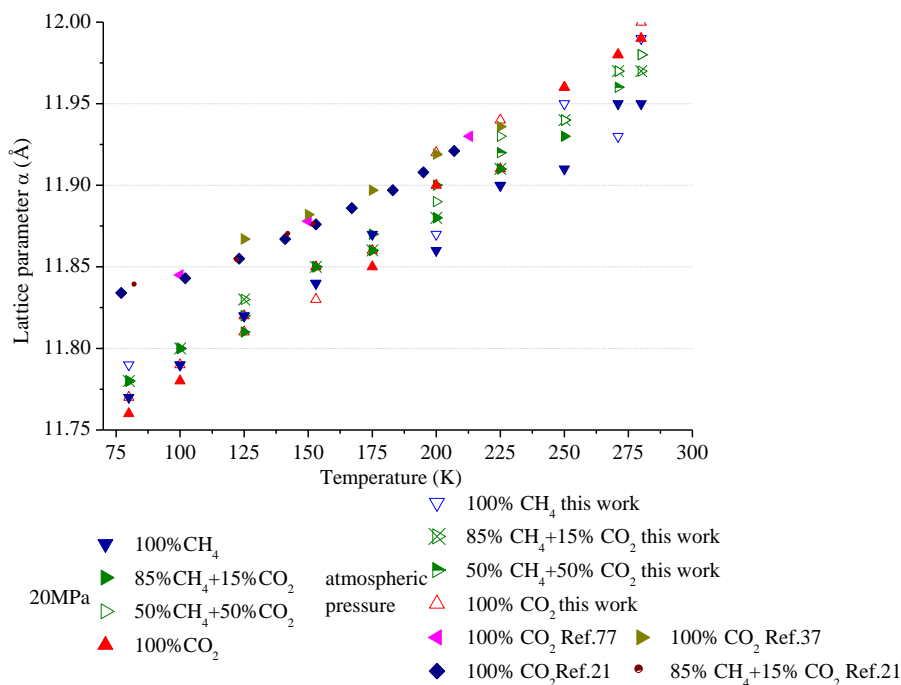


Figure 9. The lattice parameter of the  $\text{CH}_4$  and  $\text{CO}_2$  hydrates as a function of temperature at atmospheric pressure and 20 MPa compared with the experimental values.

The volumes of the unit cells under atmospheric pressure and 20 MPa as a function of temperature for different hydrates were fitted to second-order polynomials as follows:

$$\begin{aligned}
 V_{0.12\text{MPa},100\%\text{CH}_4} &= 3.5697 \times 10^{-4}T^2 + 0.2558T + 1612.8597 & (5 \leq T \leq 268 \text{ K}) \\
 V_{0.12\text{MPa},100\%\text{CO}_2} &= 3.3974 \times 10^{-4}T^2 + 0.3566T + 1600.4889 & (5 \leq T \leq 268 \text{ K}) \\
 V_{20\text{MPa},100\%\text{CH}_4} &= 3.5038 \times 10^{-4}T^2 + 0.2517T + 1610.9373 & (5 \leq T \leq 292 \text{ K}) \\
 V_{20\text{MPa},100\%\text{CO}_2} &= 3.1917 \times 10^{-4}T^2 + 0.3443T + 1599.7473 & (5 \leq T \leq 292 \text{ K})
 \end{aligned}
 \tag{11}$$

where  $V$  is the volume of the unit cell of the sI hydrate, in  $\text{\AA}^3$ , and  $T$  is temperature, in K. From these fits, the isobaric thermal expansion coefficient in each case was determined using Equation 3. Figure 10 shows the thermal expansion coefficient of the fully occupied  $\text{CH}_4$  and  $\text{CO}_2$  hydrate, obtained from the numerical differentiation of Equation 11, compared with the value given by fluctuations in the  $NPT$  ensemble (Equation 5). We observe that the value of the thermal expansion coefficient of the mixed hydrates generally increases with increasing  $\text{CO}_2$  percentage. That is, the thermal expansion of the  $\text{CO}_2$  hydrate is larger than that of the  $\text{CH}_4$  hydrate at the same temperature, especially in the high temperature region ( $>200$  K from Figure 9 in this study). This finding is in sharp contrast to an experimental report indicating that the lattice expansion of  $\text{CH}_4+\text{CO}_2$  mixture hydrates was independent of their composition<sup>21,35</sup>. This experiment may be hampered by the impurity and cage occupancy of the hydrate samples, because other measurements indicate that the thermal expansion coefficient of the  $\text{CO}_2$  hydrate is larger than that of the Xe hydrate and that of the pure  $\text{CH}_4$  hydrate at high temperature<sup>33, 36</sup>. The atomic Xe is also as symmetrical as united-atom  $\text{CH}_4$  (spherically symmetrical) in our simulations. The variation can be attributed to the strong interactions between the host and the  $\text{CO}_2$  molecules at high temperature<sup>33</sup>, which supports the idea that it is only at relatively high temperatures that the host-guest interaction plays an important role in the determination of the properties of gas hydrates (cf. the analysis of the isothermal compressibility). From Figure 10, we find that the thermal expansion coefficient is not only temperature dependent but also pressure dependent, especially at low temperatures. The variation of the thermal expansion coefficient with pressure is larger for  $\text{CO}_2$  than for  $\text{CH}_4$ . The pressure appears not to have a substantial effect on the thermal expansion coefficient at high temperatures, which may imply that the effect of the intermolecular interaction on the temperature-dependent expansion coefficient is more complex than that on the pressure-dependent compressibility. The host-host interactions may play a similarly important role with guest-host interactions in the hydrate expansion under pressure, similar to the thermal expansion behaviour observed in sII clathrate hydrate with diatomic guest molecules<sup>38</sup>. This finding is in contrast to the result that was expected<sup>28</sup> and may also explain the reason behind the difference in thermal expansion between sI and sII hydrates<sup>21</sup>.

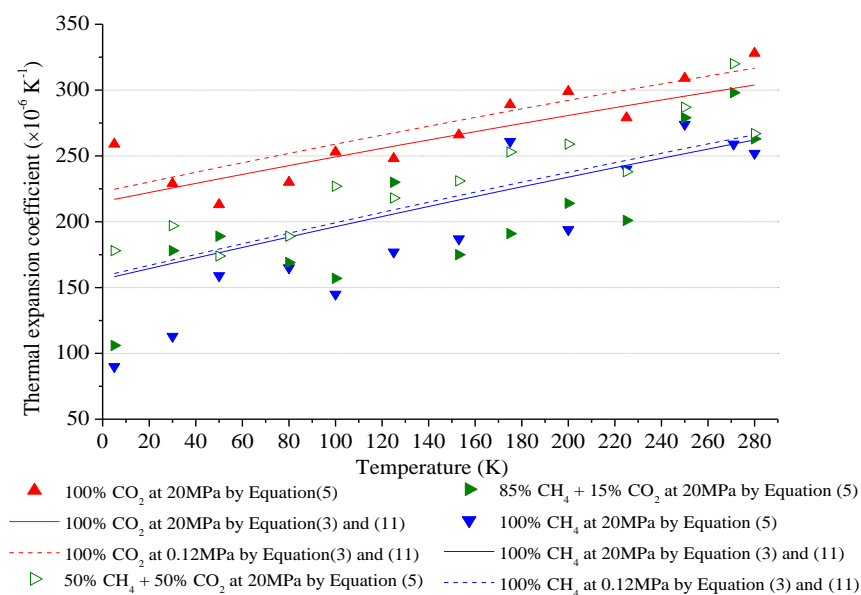


Figure 10. The isobaric thermal expansion coefficient of  $\text{CH}_4$  and  $\text{CO}_2$  hydrates as a function of temperature at 0.12 MPa and at 20 MPa.

### 3.4 Heat capacity at constant pressure

The heat capacity of a hydrate is a controlling parameter during natural gas hydrate dissociation and is especially important for the thermal dissociation of hydrates in permafrost, where the temperatures of the hydrate deposits are normally far from the equilibrium temperature<sup>6</sup>. Thus far, the specific heat capacity has been measured for CH<sub>4</sub><sup>20,39-42</sup>, C<sub>2</sub>H<sub>6</sub><sup>39,42</sup>, C<sub>3</sub>H<sub>8</sub><sup>39</sup>, Ar<sup>79</sup>, Kr<sup>80</sup>, Xe<sup>80</sup>, acetone<sup>81</sup>, ethylene oxide<sup>82-84</sup>, cyclopropane<sup>82</sup> and tetrahydrofuran<sup>84-85</sup>. There are limited data for CO<sub>2</sub> hydrates and their mixture with CH<sub>4</sub> hydrates, which is important for the replacement of CH<sub>4</sub> with CO<sub>2</sub> in hydrates and CO<sub>2</sub> sequestration in the ocean and depleted gas reservoirs. According to the discussion above (Figure 8, Figures 10), we find that the fluctuation method can give relatively similar results that are calculated by the fitting method. Therefore, the fluctuation method was also used to calculate the average heat capacities of the CH<sub>4</sub> hydrates and CO<sub>2</sub> hydrates and their mixed hydrates using MD simulations. We calculated the constant-pressure heat capacity of the mixed hydrates to be between 5-287.55 K and 10-100 MPa.

The calculated heat capacities of CH<sub>4</sub> and CO<sub>2</sub> hydrate are plotted in Figures 11 and 12 relative to published results for sI and sII hydrates. Different clathrate hydrates are observed to have relatively different heat capacities. The specific heat capacity of the mixed CH<sub>4</sub>-CO<sub>2</sub> hydrate decreases with increasing CO<sub>2</sub> percentage. Under the same temperature and pressure, the heat capacity (J.kg<sup>-1</sup>.K<sup>-1</sup>) of CO<sub>2</sub> hydrates appear to be lower than those of CH<sub>4</sub> hydrates. With increasing pressure, the heat capacities increase slightly. The heat capacity of a fully occupied CH<sub>4</sub> and CO<sub>2</sub> hydrate as a function of pressure at 271.15 K can be fitted to a line as follows:

$$\begin{aligned}
 C_{p,100\%CH_4} &= 0.16P + 2901 & (3 \leq P \leq 100 \text{ MPa}) \\
 C_{p,100\%CO_2} &= 1.51P + 2479 & (3 \leq P \leq 100 \text{ MPa})
 \end{aligned}
 \tag{12}$$

where  $c_p$  is the specific heat capacity at constant pressure, J.kg<sup>-1</sup>.K<sup>-1</sup>, and  $P$  is pressure, MPa.

According to Equation (12), the specific heats of CH<sub>4</sub> and CO<sub>2</sub> hydrates are in the range of 2902.6-2917.0 J/kg.K and 2494.1-2630.0 J/kg.K, respectively, and increase by approximately 0.4 and 5.4% at 271.15 K between 10 and 100 MPa, respectively. Waite *et al.*<sup>20</sup> performed measurements on the specific heat capacity of CH<sub>4</sub> hydrates (CH<sub>4</sub>.5.89H<sub>2</sub>O, i.e., the cage occupancy is not 100%) and reported the formula  $C_p = 3.30P + 2140$  (the units of  $C_p$  and  $P$  are the same as those in Equation (12)) at 287.55 K between 31.5 and 102 MPa (black line in Figure 11)). According to these authors, the specific heat of CH<sub>4</sub> hydrates is in the range of 2243.9- 2476.6 J/kg.K and increases by 5.9% under the above pressure conditions<sup>20</sup>.

Compared with the pressure, the effect of temperature on the specific heat is larger (Figures 11 and 12). Handa obtained approximately 887.1-2258.1 J/kg.K for CH<sub>4</sub> hydrate (CH<sub>4</sub>.6H<sub>2</sub>O, the cage occupancy of this hydrate is also not 100%) between 85 and 270 K at 3.40 MPa<sup>39</sup>. Waite *et al.* measured approximately 2040-2280 J/kg.K for CH<sub>4</sub> hydrates (CH<sub>4</sub>.5.89H<sub>2</sub>O) at 31.5 MPa between 253.15 K and 290.15 K<sup>20</sup>. These authors obtained the formula  $C_p = 6.1*(T-273.15) + 2160$  (the units of  $C_p$  and  $T$  are the same as those in Equation (13)) at 31.5 MPa between 274.15 K and 290.15 K. The heat capacity increases 11.1% within this temperature range. Nakagawa *et al.* obtained approximately 2000-2254 J/kg.K for CH<sub>4</sub> hydrate (CH<sub>4</sub>.6H<sub>2</sub>O) between 264 and 276 K at 5 MPa<sup>42</sup>. They obtained the formula  $C_p = 13.0*(T-273.15) + 2215.0$  under the above temperature and pressure conditions. The value increases 12.7% in the temperature interval of 12

K. Our simulations indicated that the heat capacity of fully occupied  $\text{CH}_4$  and  $\text{CO}_2$  hydrates as a function of temperature at 20 MPa can be approximately fitted by a line as follows:

$$C_{p,100\%CH_4} = 3.19T + 2150 \quad (5 \leq T \leq 292 \text{ K})$$

$$C_{p,100\%CO_2} = 1.70T + 2098 \quad (5 \leq T \leq 292 \text{ K}) \quad (13)$$

where  $c_p$  is the specific heat capacity at constant pressure,  $\text{J} \cdot \text{kg}^{-1} \cdot \text{K}^{-1}$ , and  $T$  is temperature, K. The average values of the heat capacity of  $\text{CH}_4$  hydrates increase approximately 14% from 2638  $\text{J}/\text{kg} \cdot \text{K}$  at 153 K to 3014  $\text{J}/\text{kg} \cdot \text{K}$  at 271.15 K.

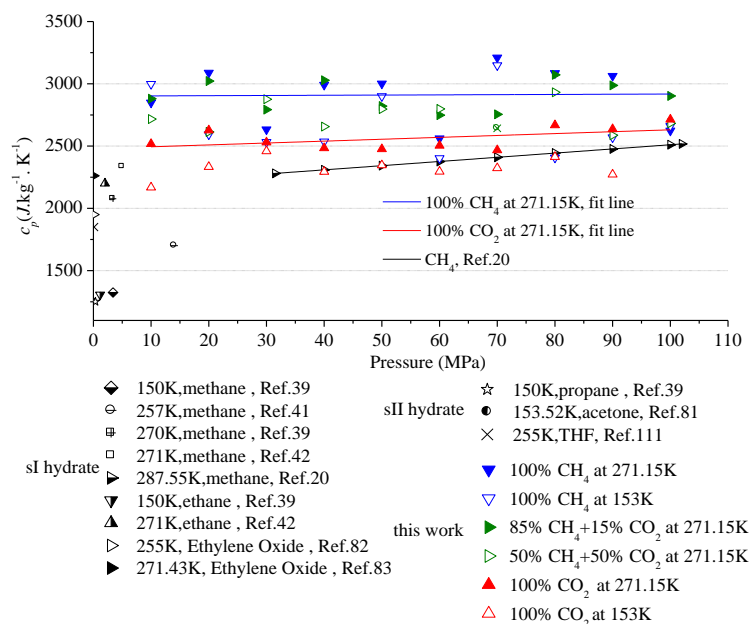


Figure 11. Pressure dependence of specific heat capacity of fully occupied  $\text{CH}_4$  and/or  $\text{CO}_2$  hydrates at 271.15 K.

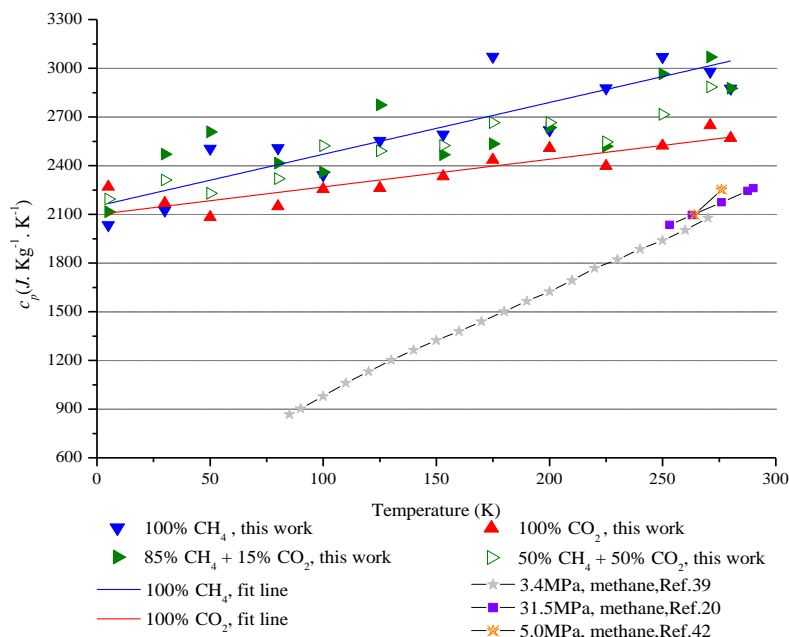


Figure 12. Temperature dependence of specific heat capacity of fully occupied  $\text{CH}_4$  and/or  $\text{CO}_2$  hydrates at 20 MPa.

Although the results yield similar dependencies on pressure and temperature, there is a systematic difference between the experimental values and the calculation of the heat capacities of CH<sub>4</sub> hydrates, especially at low temperatures. Our results for CH<sub>4</sub> hydrates are 20% higher, on average, than the results from the experiments of Waite *et al.*<sup>20</sup> and Nakagawa *et al.*<sup>42</sup> (Figures 11 and 12) and are even higher than those of other experimental reports<sup>39, 41</sup> at low temperatures. We used the same water interaction potential to calculate the compressibility, thermal expansion coefficient and heat capacity of liquid water at 298 K and 1 atm. The calculated results of compressibility and the thermal expansion coefficient agree well with the experiments. The calculated specific heat capacity of liquid water at 298 K and 1 atm is 20.23 cal/mol.K, which agrees with other calculation results<sup>86-87</sup>. However, this value is approximately 12% larger than the experimental value, 18 cal/kg.K (see the Supplementary Information).

The specific heats of CH<sub>4</sub> and CO<sub>2</sub> hydrates in this case may be similarly overestimated by 12%. The expected values were in the range of 2554.3-2567.0 J/kg.K for CH<sub>4</sub> hydrates and 2195.0-2314.4J/kg.K for CO<sub>2</sub> hydrates at 271.15 K between 10 and 100 MPa and 2593.8-2699.0 J/kg.K and 2220.0-2276.4J/kg.K at 20 MPa between 250 and 287.55 K, respectively. Without considering the temperature or pressure difference between the measurements and our simulations, the modified results are still 8% higher than the measurements made by Wait *et al.* at a higher temperature range. The experiments may have been hampered by the impurity of the hydrate samples. Although the effect of residual ice or liquid water on the measurements can be eliminated<sup>20,42,88</sup>, the residual gas is barely removed because the samples, whether synthesised in a laboratory or obtained in nature, contain many micro-pores<sup>89-91</sup>. The diameter of these pores was 100–500 nm, sometimes even 1 μm<sup>90</sup>. In addition, it is more difficult to compress polycrystalline hydrate samples with multiple pores than polycrystalline ice with multiple pores. Therefore, the micro-pores and residual gas may greatly lower the experimental values of the specific heat of gas hydrates. Furthermore, the cages in the gas hydrates in the lab and in nature may not be fully occupied by guest molecules. The cage occupancy depends upon the temperature, pressure, guest concentration and the guest and cage types. Stable sI CH<sub>4</sub> hydrates in nature contain approximately 5%-10% empty cages<sup>6</sup>. These empty cages may also affect the experimental value of the heat capacity<sup>92</sup>. Therefore, we further performed MD simulation on methane hydrates with cage occupancies normal in nature at different pressures and temperatures. The results indicated that the cage occupancy can affect the heat capacities of methane hydrates. Under the condition of a low number of empty cages (>95% occupancy), the cage occupancy of stable gas hydrates can not explain the difference in heat capacity between measurements and our simulations, regardless of temperature and pressure (Figure 13). With further decrease of cage occupancy, the heat capacities decrease slightly. The cage occupancy may then have a small effect on the heat capacities of methane hydrates under different temperatures (Figure 13a). However, the cage occupancy has a complicated effect on the heat capacities of methane hydrates under different pressures. Below 60MPa, the heat capacities seem to first increase slightly and then decrease with the decrease of cage occupancy. Above 60MPa, the heat capacities seem to first decrease slightly and then increase with the decrease of cage occupancy (Figure 13b). The extremal heat capacities of methane hydrates under different pressures may be attributed to the complicated host-guest interaction of gas hydrates under pressures, for example a possibility of phase transitions involving changes in the occupancy of cages as a function of pressure<sup>93</sup>. This interesting variation with cage occupancy will be studied further in our next work.

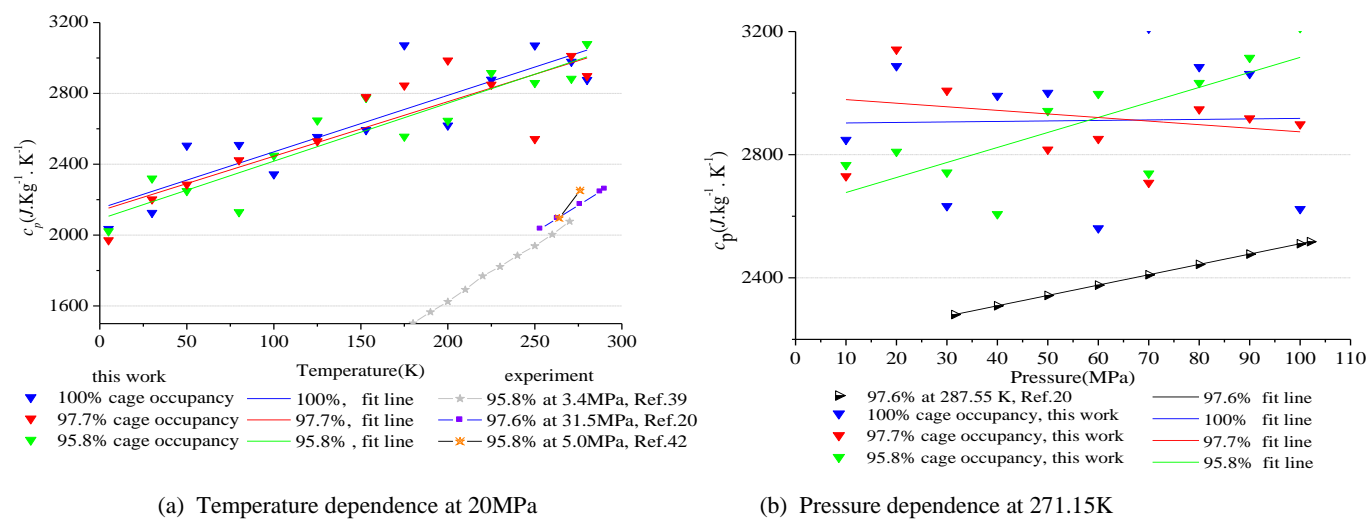


Figure 13. Specific heat capacity of CH<sub>4</sub> hydrates with different cage occupancy (95.8%-100%)

#### 4. Discussion

According to our simulations using the different water and gas molecule models, the host-host interaction and guest-host interaction both have effects on the compressibility, expansion and heat capacity of gas hydrates. However, the role of the guest-host coupling interaction appears different for the thermal and mechanical behaviours of gas hydrates. The host-host interaction plays the main role in the mechanical and thermal properties of clathrate hydrates compared to the guest-guest interaction and guest-host coupling interaction under lower temperatures (for example  $\leq 200$  K, Figure 9) and pressures (for example  $\leq 100$  Mpa, Figure 7). This is because of the elasticity of the hydrogen-bonded cages<sup>94</sup> and relatively weak host-guest interaction, which is the dominant factor governing the stability of the clathrate hydrate. In particular, the hydrogen bonds may cause unusual hydrate properties<sup>6</sup>. As observing in the experiments<sup>114</sup>, methane hydrate has measurably different strength than water ice at low temperatures (140-200 K). Under high pressure (for example  $\geq 1.0$  GPa), the guest-host coupling interaction and guest-guest interaction become so strong that the elasticity of the hydrogen-bonded cages cannot support these interactions, and structural transformation occurs<sup>61-63</sup>. However, under relatively high temperature (for example  $\geq 260$ K), the guest-host coupling interaction becomes stronger and might begin to play a significant role in the mechanical behaviour of clathrate hydrates, and the extraordinarily high strength of methane hydrate compared to other icy compounds occurs at a given strain rate<sup>95</sup>. In addition, although theory and Raman spectroscopy measurement of sI CO<sub>2</sub> hydrate indicate that CO<sub>2</sub> molecules occupy only large cavities<sup>96</sup>, more experiments and MD simulations suggest that the CO<sub>2</sub> molecules could occupy both the small and large cavities<sup>37, 97</sup>. We speculate that except for the thermodynamic competition between intermolecular interactions, the elasticity of the linear C-O bonds may be larger than the elasticity of the clathrate network of hydrogen bonds, which will cause the CO<sub>2</sub> molecules to remain in the small cages under compression conditions. In addition, we observed that at very low temperatures (e.g.  $< 125$  K), the lattice parameters of mixture hydrates decrease with increasing CO<sub>2</sub> percentage, even though the molecular size of CO<sub>2</sub> is larger than that of CH<sub>4</sub> (Figure 9). This phenomena may imply that the three site molecular description of CO<sub>2</sub> (an elongated or linear molecule) is interacting with the host cavity and with other CO<sub>2</sub> molecules (guest-guest interactions) rather than in a different manner from spherically symmetrical (atomic) CH<sub>4</sub> at very

low temperatures. More experiments and kinetic MD simulations need to be performed to investigate the effect of intermolecular interactions in large and small cages on the lattice constants of clathrate hydrates at different temperatures. The lattice parameters calculated by our simulations exhibit a discrepancy with the experimental values below 200 K (Figure 9), similar to what was observed for sH hydrates<sup>34</sup>. As a result, the calculated thermal expansivity for the hydrates is larger than the experimental values. The simulation results are close to the experimental values of ionic clathrate hydrates, including gaseous guest molecules in a similar temperature range<sup>98</sup>. Although the trend of thermal expansion with increased temperature is similar to that for the linear expansion of sI hydrates by experimental measurements<sup>21, 98</sup> (Figure 10), the calculated thermal expansion coefficients of 100% sI hydrates at atmospheric pressure in this work are much greater than the experimental values of non-ionic (the conventional gas hydrates) sI hydrates ( $\sim 70\text{--}110 \times 10^{-6} \text{ K}^{-1}$  at 180–280 K)<sup>21</sup>. The values are relatively close to those of ionic sI hydrates including gaseous guest molecules ( $\sim 110\text{--}244 \times 10^{-6} \text{ K}^{-1}$  at 180–280 K)<sup>98</sup>. In the same way, the specific heat capacities calculated by our simulations also exhibit an obvious discrepancy with the experimental values below 260 K (Figure 12). This behaviour may imply that the rigid and non-polarisable water models and guest potentials do not appear to describe the host-guest interaction or thermodynamic properties of gas hydrates well under low-temperature conditions. As mentioned above, the host-guest and guest-guest interactions are very weak because random thermal motions of the host and guest molecules are constrained under low-temperature conditions. Hydrate proton NMR analysis and dielectric constant measurements have suggested that at very low temperatures (<50 K) water molecular motion is “frozen in” so that hydrate lattices become rigid<sup>6</sup>. The reorientation of water molecules is the first-order contribution to water motion in the structure; the second-order contribution is due to translational diffusion at these low temperatures. The rate of molecular water diffusion is as much as two orders of magnitude slower in sI methane hydrate than in ice. Our supplementary calculations also indicated that at lower temperatures, a smaller number of degrees of freedom  $i$  (DOF) of water molecules in hydrates may be more suitable for determination of the heat capacity by fluctuation method, especially at solid state of water-related system (see the Supporting Information). For example, above 271.15 K,  $i=3$  can result in a  $c_p$  of water or CH<sub>4</sub> hydrate that is closer to the experimental values. However,  $i=0$  may be more suitable for ice  $I_h$  or CH<sub>4</sub> hydrate at lower temperatures and can yield a  $c_p$  value that is closer to the experimental values (Figure 14).

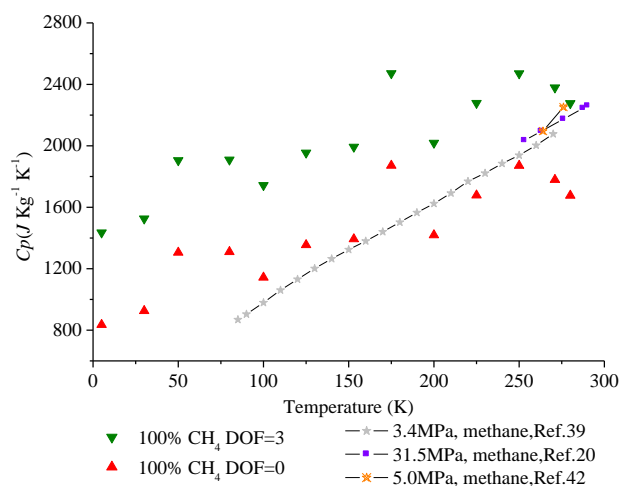


Figure 14. Temperature dependence of specific heat capacity of fully occupied CH<sub>4</sub> hydrates at 20 MPa using DOF=0 and 3.

Therefore, increasing the value of the energetic parameter of the host-guest ( $\text{CH}_4\text{-H}_2\text{O}$ ) interaction is an effective way to account for the polarisation energy between  $\text{CH}_4$  and water in nonpolarisable models at high temperatures ( $\geq 260$  K). However, this approach does not appear to simply extrapolate to low temperatures. Indeed, experiments have demonstrated that polycrystalline sI hydrates have a ductile flow<sup>88, 95</sup>, and sII hydrates exhibit an irreversible plastic-deformation-like pattern, and the expanded lattices fail to recover their original state by contraction. The tendency of thermal expansion appears to be “memorised” from previous history<sup>38</sup>. Therefore, to gain a better understanding of these properties of gas hydrates, it is necessary to use more realistic intermolecular potentials and more complex approximations that consider the anharmonic effects, although this process will require a substantial calculation time. A good description of the intermolecular interactions of the guest-guest and guest-host complexes is also important to study the properties of gas hydrates using the molecular dynamics simulations, considering the importance of the guest-host coupling interaction on the thermodynamic properties of  $\text{CH}_4$  or  $\text{CO}_2$  hydrates. A highly accurate and explicit model for the gas-water interaction potential is required, and the use of LJ parameters fitted to the *ab initio* data provides a good approach. In our further works, polarisable water models and *ab initio*-fit  $\text{H}_2\text{O-CH}_4$  or  $\text{CO}_2$  potentials will be tested by studying the effects of temperature and occupancy on the thermal and mechanical properties of monocrystalline and polycrystalline gas hydrates, and the results will be compared to those from *ab initio* density functional theory<sup>99</sup>.

## 5. Conclusions

The combination of the TIP4P2005 water model and DACNIS-UA potential can yield lattice parameters and bulk moduli of sI- $\text{CH}_4$  hydrate that are close to the experimental values and achieve a balance between relatively accurate results and low computational time. This model and potential are more appropriate for MD simulations on the isothermal compressibility of gas hydrates. This result provides a basis for studying the effect of temperature and cavity occupancy on the compressibility, expansion and heat capacity of gas hydrates by MD simulations in the future. Our MD simulations using this combination also reveal that the lattice parameter at a constant pressure or a constant temperature varies as a function of the guest type and its percentage at relatively high temperatures ( $\geq 260$  K) as well as the nature of the guest molecule (linear, symmetric, etc.). With an increase in the  $\text{CO}_2$  percentage, the lattice parameters, isothermal compressibility and thermal expansion of the hydrate increase, and the bulk modulus and specific heat capacity decrease accordingly. Therefore, the effect of the hydrate volume and heat capacity variations should not be neglected during the recovery of  $\text{CH}_4$  from  $\text{CH}_4$  hydrates in deep oceans using  $\text{CO}_2$  to replace  $\text{CH}_4$ , especially in the calculation of phase equilibria and mechanical stability of sediments.

Although the calculated thermal expansion coefficients and heat capacities of  $\text{CH}_4$  and  $\text{CO}_2$  hydrate using the fluctuation method showed a systematic deviation from the experimental values at lower temperatures, the results are still comparable with the experimental values at higher temperatures, and in reality most natural hydrate reservoirs and petroleum industry temperatures are in the higher temperature range. The present approach, which can replace the costly and time-consuming experimental measurements and be applied to calculate the variation of mechanical and thermal properties of mixture hydrates during the replacement of  $\text{CH}_4$  with  $\text{CO}_2$ , could potentially be applied to other complex hydrate systems, such as sI+sH hydrates; gas storage and transportation; and deep-sea sequestration of  $\text{CO}_2$ .

## 6. Acknowledgement

We are grateful for financial support from the Norwegian Programme for Research Cooperation with China (CHINOR) (No.208502) and Statoil ASA and Anders Jahres Fond. This work was also partly supported by the National Natural Science Foundation of China (No.51274177), the Program for New Century Excellent Talents in University (NCET-13-1013) and the Fundamental Research Funds for the Central Universities, China University of Geosciences (Wuhan) (CUG120112). The computations were carried out on the NOTUR facilities of the Norwegian Universities and computing resources in TU Delft and China University of Geosciences. Prof. Wu Jinping, Zhou Chengang and Dr. Anders Lervik are acknowledged for assistance with calculations.

## Notes and references

† Electronic Supplementary Information (ESI) available

- 1 E. D. Sloan. Fundamental principles and applications of natural gas hydrates, *Nature* 2003, **426**, 353-363.
- 2 C. Moon, R. Hawtin, P. M. Rodger. Nucleation and control of clathrate hydrates: insights from simulation, *Faraday discussions*, 2007, **136**, 367-382.
- 3 A. Ripmeester, S. T. John, C. I. Ratcliffe, B. M. Powell. A new clathrate hydrate structure, *Nature*, 1987, **325**, 135-136.
- 4 B. Tohidi, A. Danesh, A. Todd, R. Burgass. Hydrate-free zone for synthetic and real reservoir fluids in the presence of saline water, *Chemical Engineering Science*, 1997, **52**, 3257-3263.
- 5 E. D. Sloan. Introductory overview: Hydrate knowledge development, *American Mineralogist*, 2004, **89**, 1155-1161.
- 6 E. D. Sloan. C. A. Koh. Clathrate hydrates of natural gases, *Taylor & Francis/CRC Press, Boca Raton, Florida*, 2008.
- 7 J. Gudmundsson, A. Borrehaug. Frozen hydrate for transport of natural gas, *In Proceedings of 2nd International Conference on Gas Hydrate, Toulouse, France*, 1996, 439-446.
- 8 W. L. Mao, H. K. Mao, A. F. Goncharov, V. V. Struzhkin, Q. Guo, J. Hu, J. Shu, R. J. Hemley, M. Somayazulu, Y. Zhao. Hydrogen clusters in clathrate hydrate, *Science*, 2002, **297**, 2247-2249.
- 9 R. Boswell, T. S. Collett. Current perspectives on gas hydrate resources, *Energy & environmental science*, 2011, **4**, 1206-1215.
- 10 K. A. Kvenvolden. Gas hydrates—geological perspective and global change, *Reviews of Geophysics*, 1993, **31**, 173-187.
- 11 M. D. Max, S. M. Clifford. The state, potential distribution, and biological implications of methane in the Martian crust, *Journal of Geophysical Research: Planets (1991–2012)*, 2000, **105**, 4165-4171.
- 12 N. Sultan, P. Cochonat, J. P. Foucher, J. Mienert. Effect of gas hydrates melting on seafloor slope instability, *Marine Geology*, 2004, **213**, 379-401.
- 13 P. Linga, R. Kumar, P. Englezos. The clathrate hydrate process for post and pre-combustion capture of carbon dioxide, *Journal of hazardous materials*, 2007, **149**, 625-629.
- 14 Y. Bi, T. Guo, T. Zhu, S. Fan, D. Liang, L. Zhang. Influence of volumetric-flow rate in the crystallizer on the gas-hydrate cool-storage process in a new gas-hydrate cool-storage system, *Applied energy*, 2004, **78**, 111-121.
- 15 C. A. Koh. Towards a fundamental understanding of natural gas hydrates, *Chemical Society Reviews*, 2002, **31**, 157-167.
- 16 A. K. Sum, C. A. Koh, E. D. Sloan. Clathrate hydrates: From laboratory science to engineering practice, *Industrial & Engineering Chemistry Research*, 2009, **48**, 7457-7465.
- 17 F. L. Ning, Y. B. Yu, S. Kjelstrup, T. J. H. Vlught, K. Glavatskiy. Mechanical properties of clathrate hydrates: status and perspectives, *Energy & environmental science*, 2012, **5**, 6779-6795.
- 18 G. Tegze, L. Gránásy, B. Kvamme. Phase field modeling of CH<sub>4</sub> hydrate conversion into CO<sub>2</sub> hydrate in the presence of liquid CO<sub>2</sub>, *Physical Chemistry Chemical Physics*, 2007, **9**, 3104-3111.
- 19 K. S. Glavatskiy, T. J. H. Vlught, S. Kjelstrup. Toward a possibility to exchange CO<sub>2</sub> and CH<sub>4</sub> in sI clathrate hydrates, *The Journal of Physical Chemistry B*, 2012, **116**, 3745-3753.
- 20 W. F. Waite, L. A. Stern, S. H. Kirby, W. J. Winters, D. H. Mason. Simultaneous determination of thermal conductivity, thermal diffusivity and specific heat in sI methane hydrate, *Geophysical Journal International*, 2007, **169**, 767-774.
- 21 K. C. Hester, Z. Huo, A. L. Ballard, C. A. Koh, K. T. Miller, E. D. Sloan. Thermal expansivity for sI and sII clathrate hydrates, *The Journal of Physical Chemistry B*, 2007, **111**, 8830-8835.
- 22 J. S. Tse, M. A. White. Origin of glassy crystalline behavior in the thermal properties of clathrate hydrates: a thermal conductivity study of tetrahydrofuran hydrate, *The Journal of Physical Chemistry*, 1988, **92**, 5006-5011.

- 23 J. S. Tse, V. P. Shpakov, V. R. Belosludov, F. Trouw, Y. P. Handa, W. Press. Coupling of localized guest vibrations with the lattice modes in clathrate hydrates, *EPL (Europhysics Letters)* 2001, **54**, 354.
- 24 J. S. Tse, D. D. Klug, J. Y. Zhao, W. Sturhahn, E. E. Alp, J. Baumert, C. Gutt, M. R. Johnson, W. Press. Anharmonic motions of Kr in the clathrate hydrate, *Nature Materials*, 2005, **4**, 917-921.
- 25 M. Marchi, R. D. Mountain. Thermal expansion of a structure II hydrate using constant pressure molecular dynamics, *The Journal of chemical physics*, 1987, **86**, 6454.
- 26 E. J. Rosenbaum, N. J. English, J. K. Johnson, D. W. Shaw, R. P. Warzinski. Thermal conductivity of methane hydrate from experiment and molecular simulation, *The Journal of Physical Chemistry B*, 2007, **111**, 13194-13205.
- 27 H. Schober, H. Itoh, A. Klapproth, V. Chihaiia, W. F. Kuhs. Guest-host coupling and anharmonicity in clathrate hydrates, *The European Physical Journal E*, 2003, **12**, 41-49.
- 28 H. Jiang, E. M. Myshakin, K. D. Jordan, R. P. Warzinski. Molecular dynamics simulations of the thermal conductivity of methane hydrate, *The Journal of Physical Chemistry B*, 2008, **112**, 10207-10216.
- 29 A. Klapproth, E. Goreshnik, D. Staykova, H. Klein, W. F. Kuhs. Structural studies of gas hydrates, *Canadian journal of physics*, 2003, **81**, 503-518.
- 30 B. Chazallon, W. F. Kuhs. *In situ* structural properties of N<sub>2</sub>, O<sub>2</sub>, and air-clathrates by neutron diffraction, *The Journal of chemical physics*, 2002, **117**, 308.
- 31 W. F. Kuhs, B. Chazallon, P. Radaelli, F. Pauer. Cage occupancy and compressibility of deuterated N<sub>2</sub>-clathrate hydrate by neutron diffraction, *Journal of inclusion phenomena and molecular recognition in chemistry*, 1997, **29**, 65-77.
- 32 J. S. Tse. Thermal expansion of structure-H clathrate hydrates, *Journal of inclusion phenomena and molecular recognition in chemistry*, 1990, **8**, 25-32.
- 33 T. Ikeda, S. Mae, O. Yamamuro, T. Matsuo, S. Ikeda, R. M. Ibberson. Distortion of host lattice in clathrate hydrate as a function of guest molecule and temperature, *The Journal of Physical Chemistry A*, 2000, **104**, 10623-10630.
- 34 K. Murayama, S. Takeya, S. Alavi, R. Ohmura. Anisotropic lattice expansion of structure H clathrate hydrates induced by help guest: experiments and molecular dynamics simulations. *The Journal of Physical Chemistry C*, 2014, **118**, 21323-21330.
- 35 S. Takeya, T. Uchida, Y. Kamata, J. Nagao, M. Kida, H. Minami, H. Sakagami, A. Hachikubo, N. Takahashi, H. Shoji. Lattice expansion of clathrate hydrates of methane mixtures and natural gas, *Angewandte Chemie*, 2005, **117**, 7088-7091.
- 36 S. Takeya, M. Kida, H. Minami, H. Sakagami, A. Hachikubo, N. Takahashi, H. Shoji, V. Soloviev, K. Wallmann, N. Biebow. Structure and thermal expansion of natural gas clathrate hydrates, *Chemical Engineering Science*, 2006, **61**, 2670-2674.
- 37 K. A. Udachin, C. I. Ratcliffe, J. A. Ripmeester. Structure, composition, and thermal expansion of CO<sub>2</sub> hydrate from single crystal X-ray diffraction measurements, *The Journal of Physical Chemistry B*, 2001, **105**, 4200-4204.
- 38 Y. Park, Y. N. Choi, S. H. Yeon, H. Lee. Thermal expansivity of tetrahydrofuran clathrate hydrate with diatomic guest molecules, *The Journal of Physical Chemistry B*, 2008, **112**, 6897-6899.
- 39 Y. P. Handa. Compositions, enthalpies of dissociation, and heat capacities in the range 85 to 270 K for clathrate hydrates of methane, ethane, and propane, and enthalpy of dissociation of isobutane hydrate, as determined by a heat-flow calorimeter, *The Journal of Chemical Thermodynamics*, 1986, **18**, 915-921.
- 40 J. S. Livois. Development of an automated, high pressure heat flux calorimeter and its application to measure the heat of dissociation of methane hydrate, *Rice University*, 1987.
- 41 R. M. Rueff, E. D. Sloan, V. F. Yesavage. Heat capacity and heat of dissociation of methane hydrates, *AIChE journal*, 1988, **34**, 1468-1476.
- 42 R. Nakagawa, A. Hachikubo, H. Shoji. Dissociation and specific heats of gas hydrates under submarine and sublacustrine environments. In *Proceedings of 6th International Conference on Gas Hydrate, Vancouver*, 2008.
- 43 C. A. Koh, E. D. Sloan, A. K. Sum, D. T. Wu. Fundamentals and applications of gas hydrates, *Annual Review of Chemical and Biomolecular Engineering*, 2011, **2**, 237-257.
- 44 B. C. Barnes, A. K. Sum. Advances in molecular simulations of clathrate hydrates, *Current Opinion in Chemical Engineering*, 2013, **2**, 184-190.
- 45 J. S. Tse, M. L. Klein, I. R. McDonald. Dynamical properties of the structure I clathrate hydrate of xenon, *The Journal of chemical physics*, 1983, **78**, 2096-2097.
- 46 M. R. Walsh, C. A. Koh, E. D. Sloan, A. K. Sum, D. T. Wu. Microsecond simulations of spontaneous methane hydrate nucleation and growth, *Science*, 2009, **326**, 1095-1098.
- 47 P. M. Rodger. Methane hydrate: melting and memory, *Annals of the New York Academy of Sciences*, 2000, **912**, 474-482.
- 48 R. Inoue, H. Tanaka, K. Nakanishi. Molecular dynamics simulation study of the anomalous thermal conductivity of clathrate hydrates, *The Journal of chemical physics*, 1996, **104**, 9569.
- 49 L. Lundgaard, J. Mollerup. Calculation of phase diagrams of gas-hydrates, *Fluid phase equilibria*, 1992, **76**, 141-149.
- 50 A. L. Ballard. A non-ideal hydrate solid solution model for a multi-phase equilibria program, *Colorado School of Mines*, 2002.
- 51 A. L. Ballard, E. D. Sloan. The next generation of hydrate prediction IV: A comparison of available hydrate prediction programs, *Fluid phase equilibria*, 2004, **216**, 257-270.

- 52 S. Nosé A unified formulation of the constant temperature molecular dynamics methods, *The Journal of Chemical Physics*, 1984, **81**, 511-519.
- 53 W. G. Hoover. Canonical dynamics: Equilibrium phase-space distributions, *Physical Review A*, 1985, **31**, 1695-1697.
- 54 S. Melchionna, G. Ciccotti, B. L. Holian. Hoover NPT dynamics for systems varying in shape and size, *Molecular Physics*, 1993, **78**, 533-544.
- 55 F. L. Ning, K.S. Glavatskiy, T.J.H. Vlugt, S. Kjelstrup. Lattice parameters and corresponding properties of methane and Carbon dioxide hydrates: molecular dynamics simulations. 241<sup>st</sup> ACS National Meeting & Exposition, Anaheim, CA, March 27-31, 2011.
- 56 R. K. McMullan, G. A. Jeffrey, T. H. Jordan. Polyhedral clathrate hydrates. IX. Structure of ethylene oxide hydrate, *The Journal of Chemical Physics*, 1965, **42**, 2725-2732.
- 57 J. D. Bernal, R. H. Fowler. A theory of water and ionic solution, with particular reference to hydrogen and hydroxyl ions, *J. chem. Phys* 1933, **1**, 515-548.
- 58 D. Frenkel, B. Smit. Understanding molecular simulation: From algorithms to applications, *San Diego: Academic*, 1996.
- 59 A. A. Chialvo, M. Houssa, P. T. Cummings. Molecular dynamics study of the structure and thermophysical properties of Model sI Clathrate hydrates, *The Journal of Physical Chemistry B*, 2002, **106**, 442-451.
- 60 L. Y. Ding, C. Y. Geng, Y. H. Zhao, H. Wen. Molecular dynamics simulation on the dissociation process of methane hydrates, *Molecular Simulation*, 2007, **33**, 1005-1016.
- 61 I. M. Chou, A. Sharma, R. C. Burruss, J. Shu, H. K. Mao, R. J. Hemley, A. F. Goncharov, L. A. Stern, S. H. Kirby. Transformations in methane hydrates, *Proceedings of the National Academy of Sciences*, 2000, **97**, 13484-13487.
- 62 I. M. Chou, A. Sharma, R. C. Burruss, R. J. Hemley, A. F. Goncharov, L. A. Stern, S. H. Kirby. Diamond-anvil cell observations of a new methane hydrate phase in the 100-MPa pressure range, *The Journal of Physical Chemistry A*, 2001, **105**, 4664-4668.
- 63 J. S. Loveday, R. J. Nelmes, M. Guthrie, S. A. Belmonte, D. A. Allan, D. D. Klug, J. S. Tse, Y. P. Handa. Stable methane hydrate above 2 GPa and the source of Titan's atmospheric methane, *Nature*, 2001, **410**, 661-663.
- 64 J. F. Helgaker, A. Oosterkamp, L. I. Langelandsvik, T. Ytrehus. Validation of 1D flow model for high pressure offshore natural gas pipelines. *Journal of Natural Gas Science and Engineering*, 2014, **16**, 44-56.
- 65 H. Docherty, A. Galindo, C. Vega, E. Sanz. A potential model for methane in water describing correctly the solubility of the gas and the properties of the methane hydrate, *The Journal of Chemical Physics*, 2006, **125**, 074510.
- 66 M. P. Allen, D. J. Tildesley. Computer simulation of liquids, *Oxford university press*, 1989.
- 67 M. G. Martin, A. P. Thompson, T. M. Nenoff. Effect of pressure, membrane thickness, and placement of control volumes on the flux of methane through thin silicalite membranes: A dual control volume grand canonical molecular dynamics study, *The Journal of Chemical Physics*, 2001, **114**, 7174-7181.
- 68 R. Sakamaki, A. K. Sum, T. Narumi, K. Yasuoka. Molecular dynamics simulations of vapor/liquid coexistence using the nonpolarizable water models, *The Journal of Chemical Physics*, 2011, **134**, 124708.
- 69 R. Sakamaki, A. K. Sum, T. Narumi, R. Ohmura, K. Yasuoka. Thermodynamic properties of methane/water interface predicted by molecular dynamics simulations, *The Journal of Chemical Physics*. 2011, **134**, 144702-144707.
- 70 T. J. Frankcombe, G. J. Kroes. Molecular dynamics simulations of Type-sII hydrogen clathrate hydrate close to equilibrium conditions, *The Journal of Physical Chemistry C*, 2007, **111**, 13044-13052.
- 71 H. Tanaka, K. Kiyohara. The thermodynamic stability of clathrate hydrate. II. Simultaneous occupation of larger and smaller cages, *The Journal of Chemical Physics*, 1993, **98**, 8110.
- 72 J. J. Potoff, J. I. Siepmann. Vapor-liquid equilibria of mixtures containing alkanes, carbon dioxide, and nitrogen, *AIChE journal*, 2001, **47**, 1676-1682
- 73 C. Gutt, B. Asmussen, W. Press, M. R. Johnson, Y. P. Handa, J. S. Tse. The structure of deuterated methane-hydrate, *The Journal of Chemical Physics*, 2000, **113**, 4713.
- 74 V. P. Shpakov, J. S. Tse, C. A. Tulk, B. Kvamme, V. R. Belosludov. Elastic moduli calculation and instability in structure I methane clathrate hydrate, *Chemical physics letters*, 1998, **282**, 107-114.
- 75 V. R. Belosludov, T. M. Inerbaev, O. S. Subbotin, R. V. Belosludov, J. I. Kudoh, Y. Kawazoe. Thermal expansion and lattice distortion of clathrate hydrates of cubic structures I and II, *Journal of Supramolecular Chemistry*, 2002, **2**, 453-458.
- 76 A. G. Ogienko, A. V. Kurnosov, A. Y. Manakov, E. G. Larionov, A. I. Ancharov, M. A. Sheromov, A. N. Nesterov. Gas hydrates of argon and methane synthesized at high pressures: Composition, thermal expansion, and self-preservation, *The Journal of Physical Chemistry B*, 2006, **110**, 2840-2846.
- 77 T. Ikeda, O. Yamamuro, T. Matsuo, K. Mori, S. Torii, T. Kamiyama, F. Izumi, S. Ikeda, S. Mae. Neutron diffraction study of carbon dioxide clathrate hydrate, *Journal of Physics and Chemistry of Solids*, 1999, **60**, 1527-1529.
- 78 M. Helgerud, W. Waite, S. Kirby, A. Nur. Measured temperature and pressure dependence of Vp and Vs in compacted, polycrystalline sI methane and sII methane ethane hydrate, *Canadian journal of physics*, 2003, **81**, 47-53.

- 79 O. Yamamuro, M. Oguni, T. Matsuo, H. Suga. Calorimetric study on pure and KOH-doped argon clathrate hydrates, *Journal of inclusion phenomena*, 1988, **6**, 307-318.
- 80 Y. Handa, O. Yamamuro, M. Oguni, H. Suga. Low-temperature heat capacities of xenon and krypton clathrate hydrates, *The Journal of Chemical Thermodynamics*, 1989, **21**, 1249-1262.
- 81 N. Kuratomi, O. Yamamuro, T. Matsuo, H. Suga. Heat capacity and glass transition of acetone clathrate hydrate, *The Journal of Chemical Thermodynamics*, 1991, **23**, 485-494.
- 82 J. Callanan, E. Sloan. "Heat capacity measurements on structure I and II pure hydrates at low pressures and below room temperature. Final report Oct 81-Sep 82.[Tetrahydrofuran, ethylene oxide and cyclopropane hydrates]," *National Bureau of Standards, Boulder, CO (USA)*, 1982.
- 83 O. Yamamuro, Y. Handa, M. Oguni, H. Suga. Heat capacity and glass transition of ethylene oxide clathrate hydrate, *Journal of inclusion phenomena and molecular recognition in chemistry*, 1990, **8**, 45-58.
- 84 D. G. Leaist, J. J. Murray, M. L. Post, D. W. Davidson. Enthalpies of decomposition and heat capacities of ethylene oxide and tetrahydrofuran hydrates, *The Journal of Physical Chemistry*, 1982, **86**, 4175-4178.
- 85 O. Yamamuro, M. Oguni, T. Matsuo, H. Suga. Calorimetric study of pure and KOH-doped tetrahydrofuran clathrate hydrate†, *Journal of Physics and Chemistry of Solids*, 1988, **49**, 425-434.
- 86 M. W. Mahoney, W. L. Jorgensen. A five-site model for liquid water and the reproduction of the density anomaly by rigid, nonpolarizable potential functions, *The Journal of chemical physics*, 2000, **112**, 8910.
- 87 W. L. Jorgensen, C. Jenson. Temperature dependence of TIP3P, SPC, and TIP4P water from NPT Monte Carlo simulations: Seeking temperatures of maximum density, *Journal of computational chemistry*, 1998, **19**, 1179-1186.
- 88 L. A. Stern, S. H. Kirby, W. B. Durham. Polycrystalline methane hydrate: Synthesis from superheated ice, and low-temperature mechanical properties, *Energy & Fuels*, 1998, **12**, 201-211.
- 89 W. F. Kuhs, A. Klapproth, F. Gotthardt, K. Techmer, T. Heinrichs. The formation of meso- and macroporous gas hydrates, *Geophysical Research Letters*, 2000, **27**, 2929-2932.
- 90 W. F. Kuhs, G. F. Genov, E. F. Goreshnik, A. F. Zeller, K. S. Techmer, G. F. Bohrmann. The impact of porous microstructures of gas hydrates on their macroscopic properties, *International Journal of Offshore and Polar Engineering*, 2004, **14**, 305-309.
- 91 D. K. Staykova, W. F. Kuhs, A. N. Salamatina, T. Hansen. Formation of porous gas hydrates from ice powders: Diffraction experiments and multistage model, *The Journal of Physical Chemistry B*, 2003, **107**, 10299-10311.
- 92 H. Huo, Y. Liu, Z. Zheng, J. Zhao, C. Jin, T. Lv. Mechanical and thermal properties of methane clathrate hydrates as an alternative energy resource, *J. Renewable Sustainable Energy*, 2011, **3**, 063110.
- 93 S. Sasaki, T. Kume and H. Shimizu, in *Physics and Chemistry of Ice (Proceedings of 11th International Conference on the Physics and Chemistry of Ice)*, ed. W. F. Kuhs, Royal Society of Chemistry, Cambridge, 2007, pp. 529-536.
- 94 K. Morita, S. Nakano, K. Ohgaki. Structure and stability of ethane hydrate crystal, *Fluid phase equilibria*, 2000, **169**, 167-175.
- 95 W. B. Durham, S. H. Kirby, L. A. Stern and W. Zhang. The strength and rheology of methane clathrate hydrate, *Journal of Geophysical Research*, 2003, **108(B4)**, 2182.
- 96 A. K. Sum, R. C. Burruss, E. D. Sloan. Measurement of clathrate hydrates via Raman spectroscopy, *The Journal of Physical Chemistry B*, 1997, **101**, 7371-7377.
- 97 S. Hirai, K. Okazaki, S. Kuraoka, K. Kawamura. Study for the stability of CO<sub>2</sub> clathrate-hydrate using molecular dynamics simulation, *Energy conversion and management*, 1996, **37**, 1087-1092.
- 98 K. Shin, W. Lee, M. Cha, D.Y. Koh, Y. N. Choi, H. Lee, B. S. Son, S. Lee, H. Lee. Thermal Expansivity of Ionic Clathrate Hydrates Including Gaseous Guest Molecules, *The Journal of Physical Chemistry B*, 2011, **115**, 958-963.
- 99 Z.M. Jendia, A. D. Reya, P. Servio. Ab initio DFT study of structural and mechanical properties of methane and carbon dioxide hydrates. *Molecular Simulation*, 2014, DOI: 10.1080/08927022.2014.899698.